U.S. Air Force Office of Scientific Research - Grant No: AFOSR-89-0365

MESOMECHANICAL MODEL FOR FIBRE COMPOSITES: THE ROLE OF THE INTERFACE

FINAL REPORT

By M.R. PIGGOTT

Department of Chemical Engineering
and Applied Chemistry
University of Toronto, Toronto, Ontario, M5S 1A4, Canada

July 31, 1992

(U)

SECURITY CLASSIFICATION OF THIS PAGE

REPORT DOCUMENTATION PAGE

Form Approved OMB No. 0704-0188

1a. REPORT SECURITY CLASSIFICATION UNCLASSIFIED	1b. RESTRICTIVE MARKINGS
2a. SECURITY CLASSIFICATION AUTHORITY	3. DISTRIBUTION/AVAILABILITY OF REPORT Approved for public release; distribution is unlimited
2b. DECLASSIFICATION/DOWNGRADING SCHEDULE	
4. PERFORMING ORGANIZATION REPORT NUMBER(S)	5. MONITORING ORGANIZATION REPORT NUMBER(S) AFOSR TR 93-0017
6a. NAME OF PERFORMING ORGANIZATION University of Toronto 6b. OFFICE SYMBOL (If applicable)	7a. NAME OF MONITORING ORGANIZATION AFOSR/NA
6c. ADDRESS (City, State, and ZIP Code) 200 College St. Toronto, Ontario M5S 1A4 Canada	7b. ADDRESS (City, State, and ZIP Code) Building 410, Bolling AFB DC 20332-6448
8a. NAME OF FUNDING/SPONSORING ORGANIZATION AFOSR 8b. OFFICE SYMBOL (If applicable) NA	9. PROCUREMENT INSTRUMENT IDENTIFICATION NUMBER AFOSR-89-0365
8c. ADDRESS (City, State, and ZIP Code) Building 410, Bolling AFB DC 20332-6448	10. SOURCE OF FUNDING NUMBERS PROGRAM ELEMENT NO. 61102F; PROJECT NO. 2302; TASK NO B1; WORK UNIT ACCESSION NO. -

11. TITLE (Include Security Classification)

MESOMECHANICAL MODEL FOR FIBRE COMPOSITES (U)

12. PERSONAL AUTHOR(S)

Michael R. Piggott

13a. TYPE OF REPORT	13b. TIME COVERED	14. DATE OF REPORT (Year, Month, Day)	15. PAGE COUNT
Final Report	FROM 89/6/1 TO 92/5/31	92/07/31	43

16. SUPPLEMENTARY NOTATION

17. COSATI CODES			18. SUBJECT TERMS (Continue on reverse if necessary and identify by block number)
FIELD	GROUP	SUB-GROUP	
	20,11		Fibre Reinforced Polymers, Mechanics of Composites

19. ABSTRACT (Continue on reverse if necessary and identify by block number)

See Exectuve Summary (next page)

20. DISTRIBUTION/AVAILABILITY OF ABSTRACT ☒ UNCLASSIFIED/UNLIMITED ☒ SAME AS RPT. ☐ DTIC USERS	21. ABSTRACT SECURITY CLASSIFICATION UNCLASSIFIED
22a. NAME OF RESPONSIBLE INDIVIDUAL Dr. Walter Jones	22b. TELEPHONE (Include Area Code) (202) 767-0470 22c. OFFICE SYMBOL AFOSR/NA

DD Form 1473, JUN 86 *Previous editions are obsolete.*

SECURITY CLASSIFICATION OF THIS PAGE

UNCLASSIFIED

EXECUTIVE SUMMARY

This work was initially conceived as providing a theoretical framework linking microphenomena and macroscale properties in fibre composites. In addition, experimental data were to be obtained to lend substance to the theoretical constructs. Experiments were therefore carried out on the interface, and on composites which were particularly sensitive to interfacial effects, i.e. those containing short aligned fibres.

Pull out tests were used for interface studies. These showed that most fibre-polymer interphases were strong (usually stronger than the polymer) and brittle. This brittleness was an important observation which goes a long way towards explaining the properties of fibre composites containing many fibre ends.

Short aligned fibre composites were manufactured, with carbon fibres having lengths of 0.5, 1.0, 2.0 and 4.0 mm. Alignment was not perfect, nor were fibre lengths all equal to the nominal lengths, so both alignments and lengths were checked in the actual composites. Composite strengths and Young's moduli were measured and compared with predictions based on slip and shear lag theory. The agreement for moduli was moderately good, but for strengths it was very poor. Since, in addition, the stress strain plots were straight, the slip theory is not supported at all by this work. Instead, it appears highly likely that a mesomechanical theory involving crack initiation and development would work much better.

Theoretical development led to the concept of the mesostructure as a basis for mesomechanical analysis. The mesostructure was defined as adventitious small-scale structures which are present in fibre composites, but normally neglected, such as fibre waviness and uneven packing. It is shown that mesostructures can be classified, and the mechanics of them, i.e. mesomechanics, can be used to explain hitherto difficult or impossible to explain properties, such as the shear and compressive strengths of fibre composites.

1. INTRODUCTION

1.1 Mesostructures and Mesomechanics

Mesomechanics is concerned with the mechanics of materials at intermediate levels of physical dimensions [1]. At one end of the scale is micromechanics which is used to describe phenomena at the level of the grain size of metals (or ceramics) down to the level of individual atoms, and so deals with both regular and random lumpiness in materials. At the other end of the scale is continuum mechanics, in which these inhomogeneities are assumed to be smoothed out. Mesomechanics occupies the middle ground and incidentally includes the development of damage during use, and the kinematics of microstructural evolution.

Not everyone agrees that there is a need for a special term to describe micromechanics for a particular size range of lumpiness. However, in the case of fibre composites it seems particularly apt. Most workers in the field reserve micromechanics to describe the mechanical properties of the interface or interphase, and to relate these to the mechanical properties of the individual laminae that are combined to produce a high performance composite. Moreover, in the case of short fibre composites, micromechanics has been used to describe overall properties of macroscopic samples. [2]. Composite macro mechanics deals with the next scale up: the combination of laminae in a number of directions, together with honeycomb structures, etc. to make a useful piece of hardware [3].

What is assumed in all this is some perfect fibre packing (square or hexagonal) and perfectly straight fibres. This is unjustified and can have quite serious consequences. For example, there now seems little doubt that the compressive strength of carbon fibre composites is controlled by fibre waviness [4], while toughness across the grain can be enhanced by fibre bundling [5] although this, again, reduces compressive strength [6].

We will therefore use mesomechanics to describe the properties of composites containing lumpiness on a scale bigger than the fibre diameter, but excluding effects between laminae such as interlaminar shears, tensile stresses etc. The lumpiness will be referred to as the mesostructure.

1.2 The Role of the Interface

The central role played by the interface in the development of mesomechanics is apparent when we look at the compressive strength of a unidirectional fibre composite. Wavy fibres will tend to buckle much more easily than straight fibres. They are restrained by the matrix, but clearly this restraint is much reduced if the adhesion between the fibres and the matrix is weak [6] leading to a loss in compression strength [7]. Undoubtedly other properties will be similarly affected. It is therefore important that interface properties are well defined and understood. In particular we need to know how strong the interphase is, how tough it is, and whether it will fail gradually by yielding or suddenly by brittle fracture.

1.3 The Need For Experiments and Theoretical Development

The work described here falls naturally into three parts.

1. **Interface Studies.** These involved experiments designed to measure interface properties, and required the development of special techniques.

2. **Short Aligned Fibre Composites Manufacture and Testing.** Earlier work on short aligned fibre composites have not supported existing micromechanical theories very well. For example, with carbon reinforced epoxies, Young's moduli were too low and strengths were sometimes too high [8]. With glass-epoxies on the other hand strengths were usually much too low [9]. This could have been due to damage development, perhaps associated with debonding and so would have mesomechanical implications.

3. **Mesostructures** Identification of mesostructures, analysis of their effects on final properties, and consideration of manufacturing and processing implications.

These will be discussed separately.

2. EXPERIMENTS ON THE FIBRE-MATRIX INTERFACE

The single fibre pull out experiment has been adopted for this, since it permits the measurement of debonding force as a function of embedded length. This enables some

conclusions to be drawn about the nature of the interface failure mechanism, as well as giving values for debonding stress and in some cases interfacial pressure and friction as well.

2.1 Experimental Method

2.1.1. Fibre Embedment in Thermosets and low T_m Thermoplastics

A special set up has been designed and developed for the embedding of fibres, fig. 1. This is a carousel arrangement, which is used for embedding 39 fibres in one operation. Good geometry of embedment is assured by holding the fibres vertically in glass capillaries fixed inside brass tubes which can slide up and down in the upper section of the carousel. The embedment length is controlled by using a micrometer mechanism to lower the tube containing the fibre, meanwhile observing the fibre end and the resin container through a microscope.

When 39 fibres have been placed to the correct depths in the liquid resin, the whole carousel assembly is put in the oven for cure.

The process has been adapted for use with low melting temperature (low T_m) thermoplastics, by mounting the carousel on a heater. The polymer was melted, and the fibres were then lowered into small depressions made in the polymer surface.

2.1.2. Fibre Embedment in High T_m Thermoplastics

The carousel method could not be used for high melting temperature thermoplastics because of the risk of heat degradation at the melting temperature (nearly 400°C) and of oxidation. Instead, a very fast heating method was devised under a program funded by Du Pont. This involved a specially designed MicroInduction Heater, fig. 2, which would heat the specimen at up to $18^{o}Cs^{-1}$ and could reach temperatures well above the melting temperature. Heating rate, hold temperature, time at temperature, and cooling rates could be controlled very precisely, and over a wide range.

This equipment is currently being commercialized* .

The same method was used as in the carousel for fibre embedment. The resin was held in a small stainless steel container, and was heated up and melted in about 60s by the MicroInduction Heater. The temperature was then held at just above T_m while the fibre, held in a capilliary, was lowered partially into the resin, to give an embedded length of about 1 mm or less. This process took about 200s. Thereupon the MicroInduction Heater went into the controlled cool down mode. Different cooling rates were chosen to control the degree of crystallinity of the resin.

2.1.3 Fibre Pull Out

After embedment, and cure where necessary, the fibres were removed from the carousel and tested in an Instron machine. Here, special precautions were taken to ensure that the fibre stress was axial. A plate was held in the upper grip of the machine, and the fibre brought into contact with it, and then bonded to it with cyanoacrylate adhesive, see fig. 3. Pull out was carried *out at 0.5 mm min.*$^{-1}$.

For some experiments pull out was effected at elevated temperatures. For this the Instron Environmental Chamber was used. The fibres were allowed to equilibrate at the testing temperature for at least 30 min before pull out was started.

2.2. Experimental Results

2.2.1 Thermosets

Tests have been carried out with Hercules carbon fibres AS1 (unsized), AS2 (sized), AS4 (sized) and HMU in Shell epoxy resins EPON 815 and 828. For the EPON 815 the curing agent was Anchor 1170, and the curing was at temperatures in the range 60-180°C. For the EPON 828, Anchor 1115 was used, and the resin was cured at 135°C for 22 hr.

---

* **MERP Enhanced Composites, Inc., 35 Addington Avenue, Willowdale, Ontario, M2N 2L1 Canada**

Fig. 4 shows two typical room temperature pull out curves. Here the force is plotted as a function of distance pulled out. With a well adhering fibre, labelled AS4, the force increases linearly until debonding occurs. At this instant the force falls precipitately, and the remainder of the pull out is governed by friction. With a poorly adhering fibre, labelled HMU, debonding, and friction immediately thereafter, involve almost the same force, and the force is much smaller than in the well bonded case.

Fig. 5 shows the variation of debonding force with embedded length for AS4 fibres in EPON 828 cured for 22 h at 135°C. From the slope of this line and other lines from similar plots for other fibres and epoxies the mean interfacial shear strengths were estimated, and are given in Table 1. The results were frequently quite scattered, with coefficients of variation in the range 12-25%, see table 1.

HMU hardly bonds at all to epoxy resin; the frictional part of the pull out curve, see Fig. 4, gives about the same shear stress as the debonding part. This should be contrasted with the pull out curve for AS4 in the same resin (EPON 828), with the same cure, i.e. 22 h at 135°C, where the debonding force greatly exceeds the frictional force. Fig. 6 shows that F_A is not truly proportional to L: there is a small intercept, F_o. The slope corresponds to a shear stress of about 1.9 MPa. A similar conclusion emerges from results where the debonding force is less than the frictional force.

AS1, AS2, and AS4 all give about the same results when embedded in EPON 828 cured at 135°C for 22 h. Table 1. The mean and maximum debonding stresses are extremely high, i.e. up to nearly 150 MPa for the maximum and 100 MPa for the mean.

2.2.2 Thermoplastics

With nylon and polyethylene, the pull out curve shows some evidence of plastic yielding, see fig. 7. With AS4 fibres the debonding stress for polyethylene (fig. 8) is much less than for epoxy (fig. 5). There is some indication of a plateau for $L > 0.8$ mm. The average debonding stress is about 12 MPa.

With glass fibres, figs. 9 and 10, the results are very similar. All the results with thermoplastics are highly scattered, and with nylon the debonding force appears to be almost independent of embedded length (the line shown in fig. 10 indicates the debonding force vs embedded estimated for the mean shear strength from all the results shown.)

The high temperature thermoplastics developed much stronger interphases with carbon. The force-distance curves had a sudden drop when debonding occurred, indicating either ductility exhaustion or brittleness. Debonding force vs embedded length had a linear region, then a plateau, fig. 11. The effect of the sizing was not significant, fig. 12, and slow cooling the PEEK also had no significant effect.

2.2.3 Pull Out at Elevated Temperatures .

The force-distance pulled out plots, showed decreasing amounts of friction as well as some decrease in the maximum force; see fig. 13 which shows pull outs at 20°C, 50°C, 80°C and 110°C for AS4 carbon in epoxy embedded to a depth of about 100 μm. The corresponding debonding forces vs embedded length plots, fig. 14, had similar slopes, but intercepts which varied with temperature. At 110°C the intercept was anomalous, corresponding to a negative force for zero embedded length. The pulled out fibres often had quite large pieces of polymer adhering to them which had been plucked out from the surface. Their shapes were consistent with a shearing type of failure in the polymer, fig. 15. This should be contrasted with the ductile necking type of failure typical of glass pulled out of LDPE; see fig. 16. which shows four stages of the pull out process.

The shear strength of the polymer, measured at 20, 50, 80 and 110°C, using the Iosipescu shear test, did not correlate with the shear strength of the interphase, see fig. 17.

2.3 Interpretation of the Results

The interface or interphase, in the case of the epoxy, appears to be extremely strong. Tests on short cylinders of the EPON 815 indicate a compressive yield stress in the range 45-60 MPa,

with an ultimate compressive strength of 80-90 MPa. Curing at 60°C for 4 h gives much the same result as 180°C for 4 h. Thus the polymer adjacent to the interphase is expected to yield in shear at 26-35 MPa (Von Mises yield criterion). The mean interface stresses observed with EPON 815 (table 1) are 56-73 MPa with maxima as high as 100 MPa. Thus ductile failure at the interface is highly improbable with surface treated AS1 in EPON 815. This is also the case with AS1, AS2 and AS4 in EPON 828, where the interphase strength is even greater.

The lack of correlation between the interphase shear strength τ_{iu} and that of the polymer, τ_{mu}, is even more strikingly apparent when the pull out tests at elevated temperatures are considered. Fig. 17 shows that while τ_{mu} decreases rapidly with increasing temperature, τ_{iu} varies relatively little.

The debonding stress, τ_d is associated with an equivalent work of fracture in the interphase, G_i, [10], where

$$G_i = d\tau_d^2(1+\nu_m)\ln(D/d)/2E_m \qquad (1)$$

Here d is the fibre diameter, and D is the diameter of the cylinder of resin in which it had been embedded. ν_m and E_m are the Poisson's ratio and Youngs modulus of the polymer. Values of G_i associated with the debonding stresses are given in Table 1. The values for thermosets are all less than 300 Jm^{-2}, indicating that the interphase could possibly fail quite easily by brittle fracture.

The effect of fibre type is not apparently very great, at least as between AS1, AS2 and AS4, and the sizing appears to make very little difference. This needs to be confirmed however, as a comparison between sized and unsized fibres with the same type of polymer has not yet been made in the case of thermosets. The beneficial effects of surface treatment are very evident, however, when the low result from the HMU is considered.

With low temperature thermoplastics the interphase is evidently much weaker. Again, however, it is stronger than the shear strength of the polymer, τ_{mu}. For the polyethylene, this was

about 3 MPa, so the mean debonding stresses were about 400% greater in this case. Again, there are very low equivalent works of fracture (Table 1) which indicate easy failure by brittle fracture.

The high temperature thermoplastic PEEK gave a stronger interphase, but again the failure was sudden and probably brittle, with apparently quite small works of fracture, Table 1. The fibre sizing had no significant effect on the bond strength.

3. SHORT FIBRE COMPOSITES

A major emphasis of this work has been to determine whether curved stress-strain plots are produced by short aligned fibre composites, since this is a critical test of the established micromechanical theory for the failure process.

3.1. Experimental Method

A specially constructed machine [8] was used to produce aligned fibre mats. This involved dispersing the fibres in glycerine, and spreading them on the inside of a rotating cylindrical screen, fig. 18. (The rotation removed the glycerine.) Nozzle size and distance between the nozzle and the mesh had to be adjusted to suit the different fibre lengths. The drum rotated at 400 rpm and the nozzle traversed the drum at 17 mm s^{-1}.

Hercules AS2-W-12k fibres were used. They were cut to nominal lengths of 0.5, 1.0, 2.0 and 5.0 mm by Cape Composites.

Composites were made using EPON 828 with 7.0% Anchor 1115. For this, several layers of cleaned and dried mat were placed in a mold, infiltrated with the resin mixture, and then hot pressed at a pressure of no more than 3 MPa and 135°C. The final thickness of the composite was 1.5 mm for tensile and flexure tests and 3 mm for Izod tests.

Fibre lengths were checked using the microscope. At least 200 fibre lengths were measured for each nominal length. The lengths were measured both before use, and after making composites.

Fibre alignment was monitored using the method of Yurgartis [11]. This involved the cutting and polishing of sections at 5° and 10° to the main fibre direction and measuring the ellipticity of the fibre intersections. About 1200 and 500 ellipse lengths were measured for in-plane and out-of-plane distributions respectively.

For tensile testing, 20 mm x 50 mm end tabs were bonded to the specimen using epoxy. They were tested in an MTS machine at 0.5 mm min^{-1}. Flexure tests were carried out at the same rate, using 4 point bending with a gauge length of 25.4 mm and a lever arm length of 12.7 mm. Rollers were used at the loading points. For the Izod tests a Tinius Olsen Impact Tester was used.

Fibre strengths were measured by the standard method, and the interphasial shear strength was estimated from fibre fragmentation tests, as previously [8].

3.2 Experimental Results

3.2.1 Composite Quality

In-plane alignment was less good in the composites than out-of-plane; see fig. 19 which shows the results for nominally 2 mm long fibres. Fig. 20, showing the in-plane angle distributions for all the fibres used, indicates that the 2 mm fibres were the most well aligned.

Fibre lengths were not as well controlled as in the previous work [8]; significant fractions of fibres were too short, and in case of the 2 mm long fibres some were too long, see fig. 21. The nominally 5 mm fibres were nearly all 4 mm long or less, and will henceforth be designated 4 mm fibres.

The fibre strength was 2.8 ± 0.5 GPa, and the critical fibre length was 0.43, giving a critical aspect ratio of about 54.

3.2.2 Tensile and Flexural Properties

The Young's moduli of the composites made with sized fibres were somewhat less than the Rule of Mixtures values, E_{1L}

$$E_{1L} = V_f E_f + V_m E_m \qquad (2)$$

see fig. 22, the difference increasing with decreasing fibre length. Flexural moduli were slightly higher, see fig. 23.

The tensile strengths of the composites made with the sized fibres, fig. 24, were approximately linear functions of V_f. As expected for short fibre composites, strengths σ_{1u} were somewhat less than the theoretical strength for continuous unidirectional composites, σ_{1uL}

$$\sigma_{1uL} = E_{1L} \varepsilon_{fu} \qquad (3)$$

with the 2 mm fibres giving the strongest composites and the 0.5 mm fibres giving the weakest composites. Flexural strengths were higher, fig. 25, with the 4 mm long fibres giving the strongest composites and 0.5 mm giving the weakest.

The stress-strain plots for all the composites were straight lines, while for the resin the stress-strain plot was slightly curved, fig. 26. The breaking strains showed no clear trends, but all were significantly below the fibre breaking strain, and were less than one third of the matrix breaking strain, see fig. 27. The fibre strength was 2.8 ± 0.5 GPa. The critical fibre length was about 0.43 mm, giving a critical aspect ratio of about 54.

Finally when the composites were strained to 0.8% in tension (i.e. about 70% of the tensile breaking strain) before being tested in flexure, there was no apparent loss in strength, but there was some evidence of loss in flexural modulus. This loss was greatest for the shortest fibres; see fig. 28. However these results are only an indication of possible trend since the scatter of results was about equal to the differences shown on the graph.

3.3 Interpretation of the Results

The results fit in with the general trends observed previously. Thus the Young's moduli and strengths (both tensile and flexure) were roughly linear functions of V_f. The moduli, fig. 22 &

23 extrapolated to E_m at $V_f = 0$ reasonably well. The tensile strengths extrapolated to $E_m\varepsilon_{fu}$ (~ 30 MPa) fairly well also, fig. 24, as did the flexural strengths, fig. 25. However, some anomalies are apparent. The 4 mm fibres gave the highest Young's moduli and flexural strengths, but the second highest tensile strengths at most fibre volume fractions. This could only partly be explained by their less good alignment, fig. 20, since misalignments would affect flexural strengths and tensile strengths equally, while it should have a different effect on the modulus.

The imperfect alignment is allowed for in the theoretical equations as discussed previously [8]. For modulus we write

$$E_1 = \chi_1(1-\tanh(ns)/ns)V_fE_f+V_mE_m \qquad (4)$$

where

$$n^2 = 2E_m/E_f(1+\nu_m)\ln(2\pi/\sqrt{3}\,V_f) \qquad (5)$$

for fibres uniformly hexagonally packed, and with ν_m denoting the Poisson's ratio for the matrix. χ_1 (<1) represents the contributions to the modulus from the misaligned as well as the well aligned fibres. For strength we write

$$\sigma_{1u} = \chi_3\,(1-s_c/2s)V_f\sigma_{fu}+V_m\sigma_m^* \qquad (6)$$

with χ_3 (<1) representing the contribution to the strength, σ_m^* the mean matrix tensile stress at the fibre breaking strain, s is the aspect ratio, and s_c is the critical aspect ratio given by

$$s_c = \sigma_{fu}/2\tau_{iu} \qquad (7)$$

Table 2 gives the values for χ_1 and χ_3. Also given are the fibre length factors χ_2 and χ_4, compensated for the inaccuracies in the fibre cutting process

$$\chi_2 = \sum_{k=1}^{u} P_{sk} \left\{ 1\text{-}\tanh(ns_k)/ns_k \right\} \tag{8}$$

where P_{sk} is the fraction of fibres having aspect ratios $s_k \pm \Delta s$, estimated from the data shown in fig. 23, with Δs equal to one half of the intervals between the points. Also

$$\chi_4 = \sum_{k=1}^{v} P_{slk} \left\{ 1\text{-}s_c/2s_k \right\} + \sum_{k=1}^{w} P_{ssk} s_k/2s_c \tag{9}$$

where P_{slk} and P_{ssk} being the fractions as above for longer ($s>s_c$) and shorter ($s\leq s_c$) fibres.

It can be seen that χ_1 and χ_3 differ somewhat, and the better alignment of the 2 mm fibres shows up as higher values of χ_1 and χ_3 (Table 2.).

However, our trends, as indicated in figs 22 and 24, when used to check the theoretical expressions, show poor agreement. For the experimental results we write, for modulus

$$E_1 = A_E V_f E_f + V_m E_m \tag{10}$$

and for strength

$$\sigma_{1u} = (A_s V_f E_f + V_m E_m)\varepsilon_{fu} \tag{11}$$

We use the lines shown on figures 23, 24 and 25 to estimate A_E and A_S

Comparing equations 4 and 6 with 10 and 11, agreement between theory and experiment requires $A_E = \chi_1\chi_2$ and $A_S = \chi_3\chi_4$. It is apparent from Table 2 that agreement is not very good. The comparisons are shown graphically in figs. 29 and 30.

The modulus results are a little above theoretical estimates, whilst the earlier Sanadi [8] results, which are also shown in the figures are about right, see fig. 29. The glass fibre results of Chuang [9] fall into two groups; the 3 mm and 6 mm fibres give high results, while the 1.6 and 0.8 mm fibres give low results. These low results may have been because the fibres were milled. This severely damaged the fibres, which may have affected the effective length distributions, since badly cracked fibres could well have broken during processing.

The strength results were all somewhat higher than the theoretical estimates, fig. 30, with some of the flexural results being extremely high (especially those for the 4 mm fibres, which had $A_s = 0.83$ for flexure). The earlier Sanadi results [8] are about as far above the theoretical line as the tensile results reported here. These composites had $\varepsilon_{fu} \cong \varepsilon_{mu}/3$ (Ko) and $\varepsilon_{fu} \cong \varepsilon_{mu}/4$ (Sanadi). The glass fibre composites (Chuang) [9], which had $\varepsilon_{fu} \cong 2.4\ \varepsilon_{mu}$, gave very low results, especially when the milled fibres were used ($A_s = 0.3$ and 0.4).

A major problem with this type of experiment is the difficulty of producing high quality specimens with fibres all the same lengths and aligned consistently, with fibre volume fractions well controlled and with the fibres uniformly distributed. Large resin rich areas are a particular problem at low fibre volume fractions. Inevitably the results tend to be scattered and interpretation is therefore somewhat difficult.

The most important clues to the behaviour of these short fibre reinforced polymers are the straightness of the stress strain curve, and the breaking strains.

1. Straight stress-strain curves indicate that progressive slip does not take place. Hence, equation 6 cannot explain the behaviour of these short fibre composites, and consequently the theory on which it is based is not supported by these experiments.

2. The breaking strains of the composites investigated here were always less than the fibre breaking strains. Thus, again, equation 6 is not supported.

The breaking strains for the glass-epoxies mentioned earlier [9] are even lower. They are shown in fig. 31, and, as expected since $\varepsilon_{mu} < \varepsilon_{fu}$, are much less than the fibre breaking strain. They are also, more surprisingly, much less than the breaking strain of the polymer for the low

volume fraction results with the 3 mm and 6 mm long fibres (aspect ratios about 170 and 330). The shorter fibres (0.8 and 1.6 mm long) have very low breaking strains at all fibre volume fractions.

In view of these striking divergencies from the theoretical predictions, we may need to abandon the concept of the critical fibre aspect ratio for reinforced plastics and re-think the basic theory. This was founded on ideas borrowed from metals which yield and then flow at a stress which is often assumed to be approximately constant. Polymers are different. Fig. 32 compares the model [12] and recent work using Laser Raman Scattering [13]. Further evidence comes from the study of the ceramic-polymer interface using the single fibre pull out method. The model was based on ductile metal behaviour involving very short embedded lengths (< 10 diameters) [14]. However, the actual behaviour of the carbon-epoxy interface is brittle as shown in figs. 4 and 13. There is now a body of evidence not only that this interface is brittle but also that it has properties which are totally unrelated to the shear strength of the polymer, see fig. 17, and note that these results are supported by the studies of Netralvali et al [15] using a different test and different polymers. In addition, evidence has recently appeared which suggests that a high modulus (and presumably high strength) form of polymer may possibly be present at the ceramic-polymer interface [16, 17].

At this time it is only possible to speculate on the failure processes which trigger composite failure. Any theory will have to be consistent with the following.

1) For well bonded systems with $\varepsilon_{fu} << \varepsilon_{mu}$ the failure strain is not a function of fibre length (except possibly with very short fibres, i.e. s < 100). Since the Young's modulus is approximately given by the shear lag theory (after due allowance has been made for misaligned fibres), the strength is given by $\sigma_{1u} = E_1\varepsilon_{fu}$ with

$$E_1 = \chi_1^*(1-\frac{\tan(ns)}{ns})V_fE_f + V_mE_m \qquad (12)$$

at the lower fibre volume fractions (≤ 0.2) and somewhat less than this at higher V_f's.

It seem highly probable that some debonding of misaligned fibres occurs either at very low applied stresses, or even before any stress is applied, as a consequence of cure shrinkage stresses. This would reduce χ_1 and account for the reduced modulus indicated by the Sanadi results with the shortest fibres (2 mm & 1 mm) [8]. Hence we use a modified χ_1, which we have written as χ_1^*.

2) For well bonded systems with $\varepsilon_{fu} \sim \varepsilon_{mu}/3$ (the case examined here) the composite breaking strains are in the range 0.6 ε_{fu} to 0.9 ε_{fu} for the longer fibres ($s > 100$) with very little effect due to volume fraction. For very short fibres ($s < 100$) the breaking strains are $\sim \varepsilon_{fu}/2$. Equation 4 gives the approximate modulus, E_1 while for strength we write

$$\sigma_{1u} = E_1 \varepsilon_{1u} \tag{13}$$

In this case ε_{1u} must be measured. Its low value is probably due to cracks developing from fibre debonds near the fibre ends. We would expect a fibre volume fraction effect, since the number of fibre ends in an aligned fibre composite lying within one fibre diameter of any given cross section normal to the fibres is

$$N_e = 4V_f/\pi d^2 s \tag{14}$$

per unit area . If each fibre end produces a cracked area A_c which is proportional to the fibre cross section, i.e. $A_c = A_o \pi d^2/4$, where A_o is a constant then

$$A_c = 4A_o V_f/s \tag{15}$$

So we would expect also to have a fibre aspect ratio effect. These effects must be quite small in the case examined here because there were no clear trends in the breaking strains, fig. 16. However, the V_f effect is apparent in the Sanadi results [8].

3) For well bonded systems with $\varepsilon_{fu} > \varepsilon_{mu}$ (i.e. glass fibre reinforced epoxies and polyesters) ε_{1u} is probably a monotonically increasing function of fibre volume fraction, fig. 31,

and is affected by the fibre aspect ratio. Thus we do not have agreement with equation 15 since the equation suggests an increase in possible cracks with increasing fibre volume fraction. Instead, crack size might be important. Thus, at low fibre volume fractions, large matrix cracks can develop in resin rich regions. These might perhaps develop significant stress concentrations, and be able to continue across adjacent fibres, leaving these fibres bridging the cracks, and thus able to debond and pull out without fracturing.

More work is clearly needed on the actual failure process, with careful experiments to determine at what stage matrix cracking starts. These experiments should perhaps include acoustic emission studies to detect debonds and cracks. That polymer cracks can form near fibre ends is well known [8].

Further theoretical work on the effect of fibre ends and breaks, such as that carried out by Curtis [18] should also be pursued; however closed form expressions are preferable to numerical analysis. In particular a mesomechanical theory of crack development is needed.

4. THEORETICAL DEVELOPMENTS

The key to the development of mesomechanics may well lie in a better understanding of the substructures involved. Heretofor it has been almost universally assumed that a two step approach could be used: i.e. 1) from micromechanics directly to lamina and then 2) from lamina to laminate properties. That this is probably erroneous is apparent when we look at the prediction of compressive strength . Efforts to do this on the basis of the simple micromechanical approach [19] have been unsuccessful [6]. Instead, a major contribution to compressive failure comes from lack of perfect fibre alignment, and there is a direct correlation between fibre alignment and strength and modulus in compression [4]. However, prediction of compressive strength may also require inclusion of fibre bundle effects [6].

Fibre waviness and fibre bundles constitute substructures which are not normally intended to be present in a composite. We will call such substructures mesostructures.

4.1 Mesostructures

Mesostructures will be defined here as structures which are coarser than the fibre-interface-polymer microstructure, but on a finer scale than the lay-up, core-skin structure and outer form of the material. They are generally a fortuitous structure, i.e. not part of the original design.

At least two classes of mesostructure can be identified, since we can have disorder in what is intended to be a rigidly ordered structure, and conversely, order in what is intended to be a disordered structure. Within each class there are at least two types of order/disorder: orientation effects and packing effects. We will discuss the two classes separately.

4.2 Adventitious Disorder

4.2.1 Orientation Errors

Even in the best laid up laminates it is impossible to ensure that the fibres are perfectly straight, yet perfect straightness is assumed in practically all theoretical treatments of fibre composites. This lack of straightness shows up as imperfect alignment or a fibre waviness. This will directly affect the compressive strength (and modulus), shear strength, delamination resistance, and fatigue endurance (including tension-tension fatigue). There may also be secondary effects on tensile modulus and strength, and fracture toughness. Local misorientations can be quantified using the method of Yurgartis [11] but fibre waviness is more difficult to measure [20].

4.2.2 Packing Faults

Normally, theoretical treatments assume hexagonal packing of fibres in three dimensional aligned fibre structures, although square packing is sometimes assumed. Laminates are treated theoretically as though, in each lamina, there is a single layer of fibres, equispaced, and with axes located on the centre plane of the lamina. Real composites, on the other hand, contain resin rich areas which are relatively weak, and resin poor areas where contacts can occur. The most serious example of packing faults, moreover, is the lack of either fibre or resin in some regions, i.e. voids in the structure. All composites appear to contain voids.

The main effect of these faults will be to reduce the various strengths of a composite: tensile, compressive, shear etc. However, if the composite contains excessive voids (a good composite has roughly one volume per cent of them) the moduli could also be affected.

4.3 Adventitious Order

4.3.1 Orientation Effects

In a random mat or a sheet molding compound, the orientation of the fibres is seldom completely random, although normally complete randomness is usually intended. The process of molding these materials can also develop preferred orientations. These will give the composite unexpectedly high properties in some directions, and correspondingly low properties in others. Similar effects are observed when short fibre reinforced thermoplastics (e.g. nylon) are molded. The orientation of the fibres inside the molding is complex, and reflects the flow pattern. For example, in thin sections the fibres are usually preferentially oriented parallel to the plane of the mold surfaces. Design data for such moldings must take these mesostructures into account.

4.3.2 Packing Effects

In short fibre composites, the fibre ends are expected to be positioned at random. However, imperfect dispersion can result in some end synchronization, i.e. fibre ends may be concentrated in (or close to) particular planes. This will weaken the composite. In continuous and in long fibre composites fibre bundling can occur. In this case fibre bundles (perhaps from the original roving or tow; especially if it sustains a little twist) retain their presence in the composite, and act in harmony. This can increase the across-the-grain toughness of a composite, and reduces the compressive strength.

4.4 Prediction of Properties Using Mesomechanics

This already appears to be possible in the case of compressive strength, and some progress has been made in fatigue of carbon fibre composites [21]. Further developments will require a

much greater attention to details of the mesostructure.

The concept of mesostructures has been applied to shear strength. The "classical" theory for shear strength assumes straight and uniformly arranged fibres, separated by polymer. The theoretical shear strength is, therefore, expected to be equal to the shear strength of the weakest component, i.e. the polymer. Experimental values for shear strength are somewhat greater than this [22].

The reason for this discrepancy is apparent when the actual structure of fibre composites is examined. The fibres are never entirely straight, and this requires the crack plane to deviate, or else fibres cross the crack plane, and must be broken in order for shear failure to occur. If the volume fraction of fibres crossing the cracks plane is V_{fb}, then the shear strength of the composite τ_{13u} is given by

$$\tau_{13u} = V_{fb}\sigma_{fu}/2+(1-V_{fb})\tau_{mu} \qquad (16)$$

Fibre bridging appears to be the most likely contributor to the extra shear strength (over and above that of the polymer) but one other mesostructure that may be important is fibre bunching. This causes deviations of the failure plane, increasing its surface area.

In the case of the short fibre composites studied here we need to examine orientation errors, packing faults (especially voids) and fibre end synchronization. The first step here will be an attempt to quantify them.

5. CONCLUSION

5.1 The Fibre Matrix Interface

Pull out tests suggest that interphases between fibres and polymers are almost universally strong, and often stronger than the polymer. The only exception observed in these experiments was the high modulus carbon, Hercules HMU, which appeared not be adhere to epoxies at all. The interphase properties appeared to be unrelated to those of the polymer and in particular, when the testing temperature was raised the interphase strength changed very little while the polymer

shear strength dropped sharply. Furthermore, most interphases appeared to be very brittle, with works of fracture much less than those of the polymer.

5.2 Short Aligned Fibre Composites

These obey mixture rule type expression quite well for Youngs modulus, but less well for strength. Flexural strengths were greater than tensile. The strengths could not be reconciled with the interface yielding and slip theory, and since the stress strain plots were straight until composite failure, the work provided no support for the theory.

It is possible that cracks, starting at the fibre-matrix interface near fibre ends, initiates a multiple fracture type of failure process. Such a mechanism could involve only very small inelastic strains, and help explain the straightness of the stress-strain plots. However, the evidence for a critical damage strain was not very great. Further work is therefore needed on the strains needed to initiate damage, especially fibre debonding and matrix cracking near fibre ends. Experiments with *single short length fibres embedded in polymers* should provide the necessary data. In addition, further work on crack development should be carried out, and a mesomechanical analysis would be appropriate..

5.3 Advances in Mesomechanical Theory

The concept of the mesostructure, and mesomechanics as the mechanics thereof, seems particularly apt for fibre composites. This is because composites have a range of hitherto neglected structures. Furthermore these mesostructures can be used to help explain properties, such as compressive and shear strength, which have been difficult or impossible to predict from constitutent material properties. The mesostructure also provides a link between processing in the manufacture of fibre composites and their final properties.

6. REFERENCES

1. G.K. Haritos, J.W. Hager, A.K. Amos and M.J. Salkind, Int. J. Solids Structures 24, (1988), 1081.

2. M.R. Piggott, "Load Bearing Fibre Composites", (Pergamon, Oxford, 1980), Chpt. 4.

3. J.E. Ashton, J.C. Halpin and P.H. Petit, "Primer on Composite Materials: Analysis", (Technomic, Westport, Conn. 1969)

4. A. Mrse and M.R. Piggott, Proc. of 36th Int. SAMPE Symp., (1990), 2236.

5. M. Fila, C. Bredin, and M.R. Piggott, J. Mater Sci. 7, (1972), 983.

6. M.R. Piggott, J. Mater Sci. 16, (1981), 2837.

7. N.L. Hancox, J. Mater Sci 10, (1975), 234.

8. A.R. Sanadi and M.R. Piggott, J. Mater Sci. 20, (1985), 421.

9. H.Y. Chuang and M.R.Piggott, Proc. of Amer. Soc. for Comp., (1990), 984.

10. M.R. Piggott, Comp. Sci. Tech. 42, (1991), 57.

11. S.W. Yurgartis, Comp.Sci. Tech. 30, (1987), 279.

12. D. Hull, "An Introduction to Composite Materials" (Cambridge Univ. Press, 1981), 201.

13. C. Galiotis, Comp.Sci. Tech. 42, (1991) 125-150.

14 W.R. Tyson, Ph.D. Thesis, Cambridge, University of Cambridge, (1964), p. 80.

15. A.N. Netravali, R.B. Henstenburg, S.L. Phoenix and P. Schwartz, Polymer Comps. 10, (1989), 226.

16. P.H.T. Vollenberg and D. Heikens, Polymer 30, (1989), 1656-62.

17. P.H.T. Vollenberg, L.J.M. Van deVen and D. Heikens, Polymer 30, (1989), 1663-8.

18 P.T. Curtis, Comp. Sci. Tech. 27, (1986), 63-86.

19. B.W. Rosen, "Composite Materials", (American Soc. for Metals, Ohio, 1964), Chp.3.

20. A.L. Highsmith, J.J. Davies and K.L.E. Helms, ASTM STP 1120, (1992), 20.

21. M.R. Piggott and P.W.K. Lam, ASTM STP, 1110, (1991), 686.

22. C.A. Dostal (ed), "Composites: Engineered Materials Handbood" (ASM Int. Ohio, 1987), 1, 376.

7. STUDENTS TRAINED

Four graduate students have been working on this project, and two have written their work up and have been awarded M.A.Sc.'s.

9. PUBLICATIONS

Four papers have been prepared which come directly from this contract.

1. **M.R. Piggott**, "Mesostructure in Fibre Composites", CANCOM '91, Montreal, Sept. 4, 1991.

2. **M.R. Piggott**, "Fibre Composites: Mesostructure & Mesomechanics", IUTAM Symp., Blacksburgh, VA, Oct. 29-30, 1991.

3. **M.R. Piggott,** "Mesostructures - an Overview", Proc of 37th Int. SAMPE Symposium, Anaheim, CA, Mar. 9-12, 1992.

4. **M.R. Piggott, M. Ko and H.Y. Chuang**, "Aligned Short Fibre Reinforced Thermosets: Experiments and Analysis Lends Little Support for Established Theory", Paper presented at Microphenomena in Composites Meeting, Herzlia, Israel, June 28 - July 1, 1992. Submitted for publication in Comp. Sci. Tech..

Eight papers have been prepared on work partially supported by this contract.

1. **Z-N Wang and M.R. Piggott**, "Relations Between Polymer & Fiber - Polymer Interfaces Properties, Proc of American Society for Composites, Albany, N.Y, 1991, 725.

2. **M.R. Piggott and P.W.K. Lam**, "Fatigue Failure Processes in Aligned Carbon Epoxies, ASTM STP 1110, pp 686-95, (1991).

3. **M.R. Piggott**, "Failure Processes in the Fibre-Polymer Interphase", Comp. Sci. Tech. 42, 59-78, (1991).

4. **M.R. Piggott,** "The Single Fibre Pull Out Method: Its Advantages, Interpretation and Experimental Realization", ICCI-IV Conference, Cleveland, OH, May 26-29, 1992. Submitted to Composites Interface.

5. **M.R. Piggott,** "Tailored Interphases in Fibre Reinforce Polymers", Materials Research Society, Savannah, GA, Feb. 18, 1990, 22.

6. **H.Y. Chuang and M.R. Piggott**, "Properties of Short Aligned Glass Fibre Reinforced Epoxies", Proc. of Amer. Soc. for Comp., Lansing, MI, June 10, 1990, 984.

7. **M.R. Piggott,** "Micromechanics of Interfaces, IPCM '91, Belgium, Sept. 17, 1991, 3.

8. **A. Mrse and M.R. Piggott,** "Mechanisms of Compressive Failure in Fibre Composites", 1st International Conference on Deformation and Fracture of Composites, Manchester, U.K. March 25, 1991, 1-20.

In addition, the concepts developed here have influenced the interpretation of the results of work which was ongoing in the Advanced Composites Physics & Chemistry Group at the time this contract started. In particular the concept of mesostructures appears in the following papers which have been accepted or are being submitted for publication.

1. **A. Mrse and M.R. Piggott,** "Compression Properties of Unidirectional Carbon Fibre Laminates: I: A Compact Flexure Beam For Compression Testing, Accepted by Comp. Sci. & Tech. 1992.

2. **A. Mrse and M.R. Piggott,** "Compression Properties of Unidirectional Carbon Fibre Laminates: II: The Effects of Unintentional and Intentional Fibre Mislignments, Accepted by Com. Sci. & Tech. 1992.

3. **D. Loken and M.R. Piggott,** "Mesostructures and the Tensile Strength of Aligned Fibre Composites", to be submitted, J. Comp. Tech. Res., Aug. 1992.

4. **D. Loken and M.R. Piggott,** "Mesostructures and the Fatigue Endurance of Aligned Fibre Composites", to be submitted, J. Comp. Tech. Res.., Aug. 1992.

ACKNOWLEDGEMENTS

The author would like to express his thanks to Lt. Col. G. Haritos for introducing him to the concept of mesomechanics. This led to the idea of mesostructures, and the initiation of a series of conferences on Mesostructures and Mesomechanics in Fibre Composites, starting May 17 & 18, 1993.

TABLE 1.

DEBONDING DATA FROM PULL OUT EXPERIMENTS

Fibre	Resin	Cure Temp. (°C)	Time (h)	Debonding Stress (MPa) Maximum	Debonding Stress (MPa) Mean**	Work of Fracture (Jm^{-2})
AS1*	815	100	0.5	76	56 ± 71	38
AS1*	815	180	0.5	83	61 ± 11	45
AS1*	815	60	4	72	59 ± 11	42
AS1*	815	180	4	100	73 ± 18	64
HMU	828	135	22	8	2.9 ± 1.3	
HMU+	828	135	22	2.3	1.7 ± 0.3	
AS1	828	135	22	146	100 ± 19	120
AS2	828	135	22	139	84 ± 24	85
AS4	828	135	22	119	88 ± 11	93
AS4	LDPE			28	12 ± 5	16
Glass	LDPE			29	13 ± 4	18
Glass*	LDPE			13	12 ± 1	16
Glass	Nylon 12			49	18 ± 10	10
AS4*	PEEK	-	-	116	90 ± 30	73
AS4	PEEK	-	-	175	85 ± 20	66

* Unsized fibres + Frictional Results ** ± One standard deviation

TABLE 2

CONSTANTS FOR THE MODULI AND STRENGTHS OF SHORT IMPERFECTLY ALIGNED FIBRE COMPOSITES

Fibre Length (mm)	Modulus Constants χ_1	χ_2	$\chi_1\chi_2$	A_E	Strength Constants χ_3	χ_4	$\chi_3\chi_{42}$	A_S
0.5	0.48	0.72	0.36	0.44	0.32	0.49	0.16	0.41
1.0	0.61	0.88	0.54	0.70	0.41	0.72	0.30	0.47
2.0	0.64	0.91	0.58	0.73	0.43	0.84	0.36	0.59
4.0	0.62	0.96	0.60	0.86	0.42	0.91	0.38	0.57

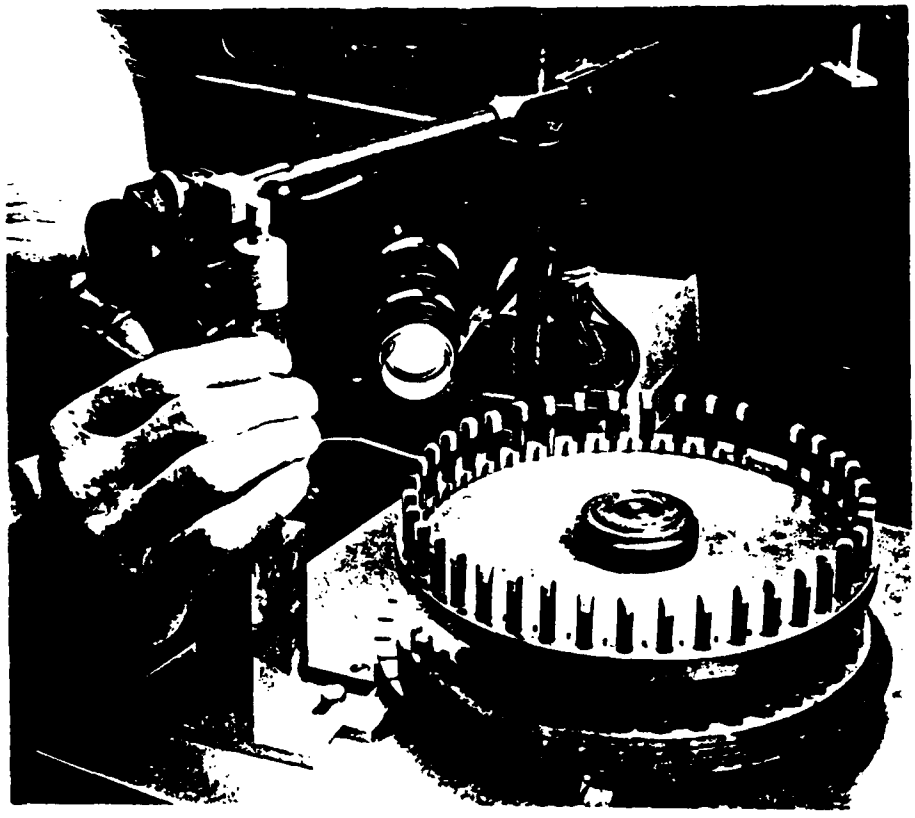

Fig. 1. Set up used for embedding fibres in thermosets and low T_m thermoplastics.

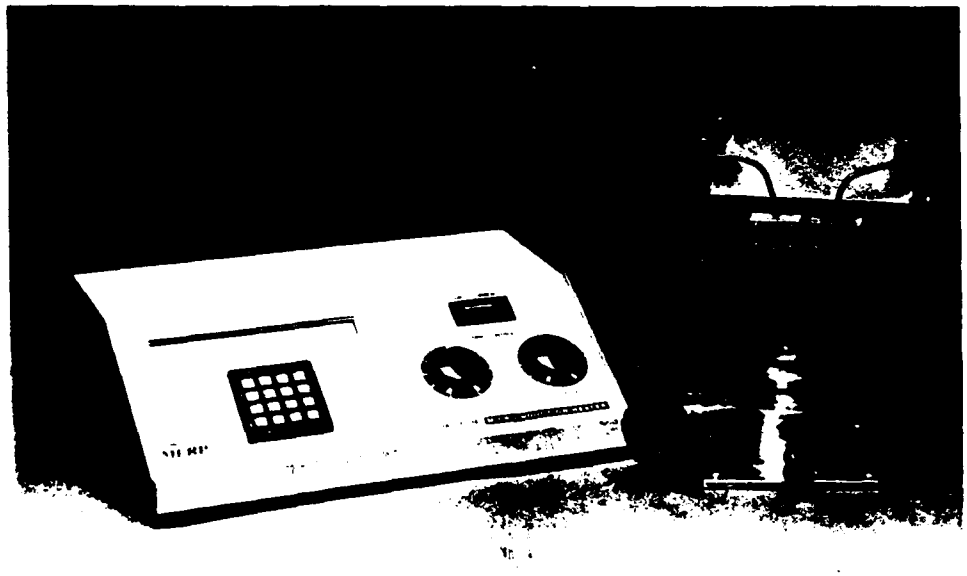

Fig. 2. MicroInduction Heater set up for embedding fibres in high T_m thermoplastics.

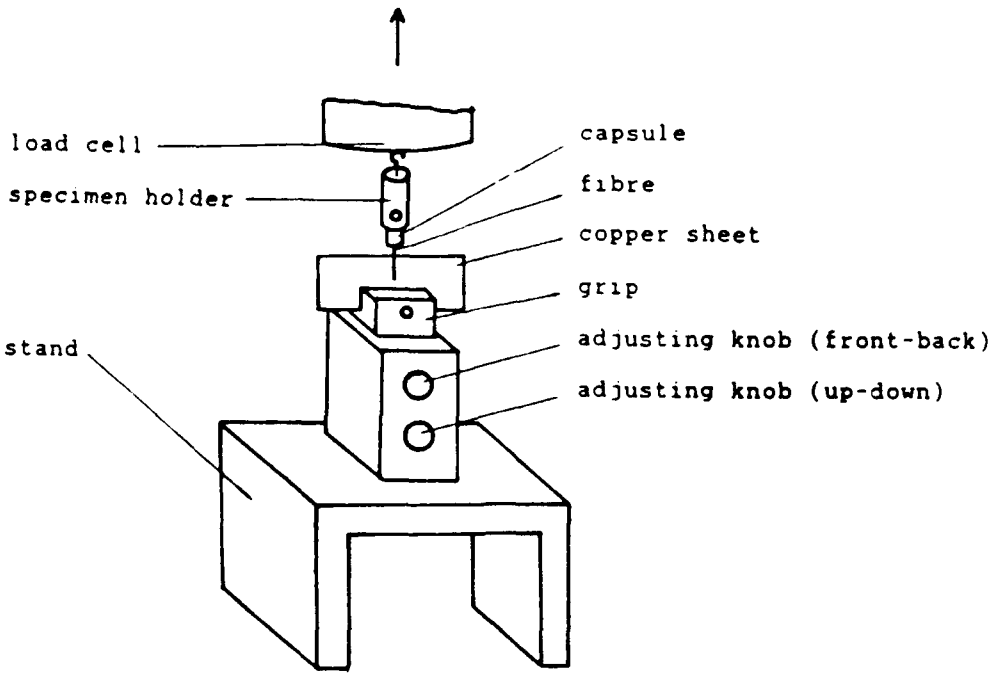

Fig. 3. Pull out test set up.

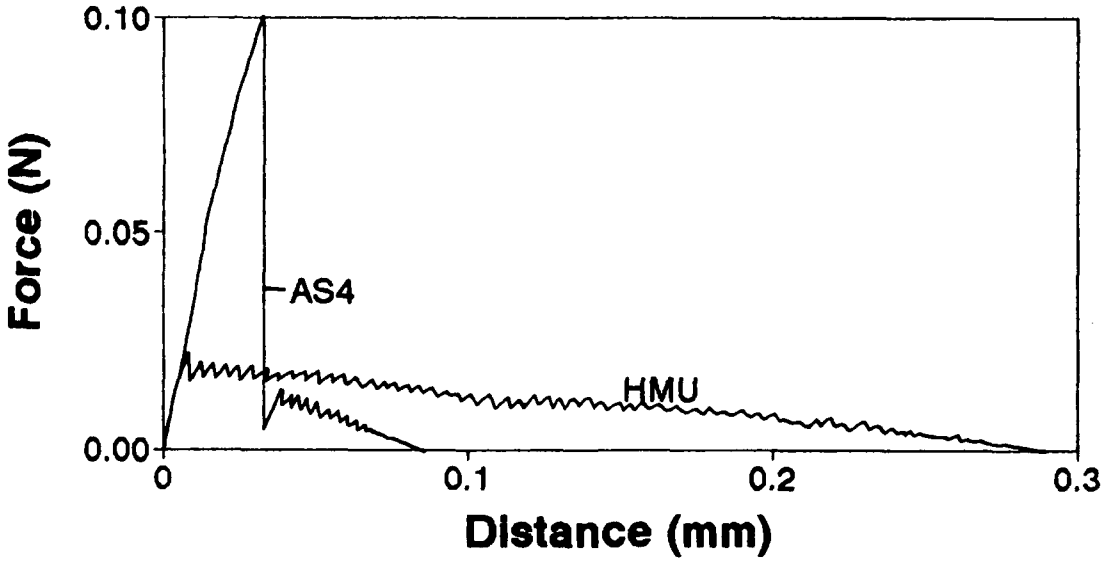

Fig. 4. Force vs distance moved during pull out. HMU and AS4 fibres embedded in EPON 828 epoxy.

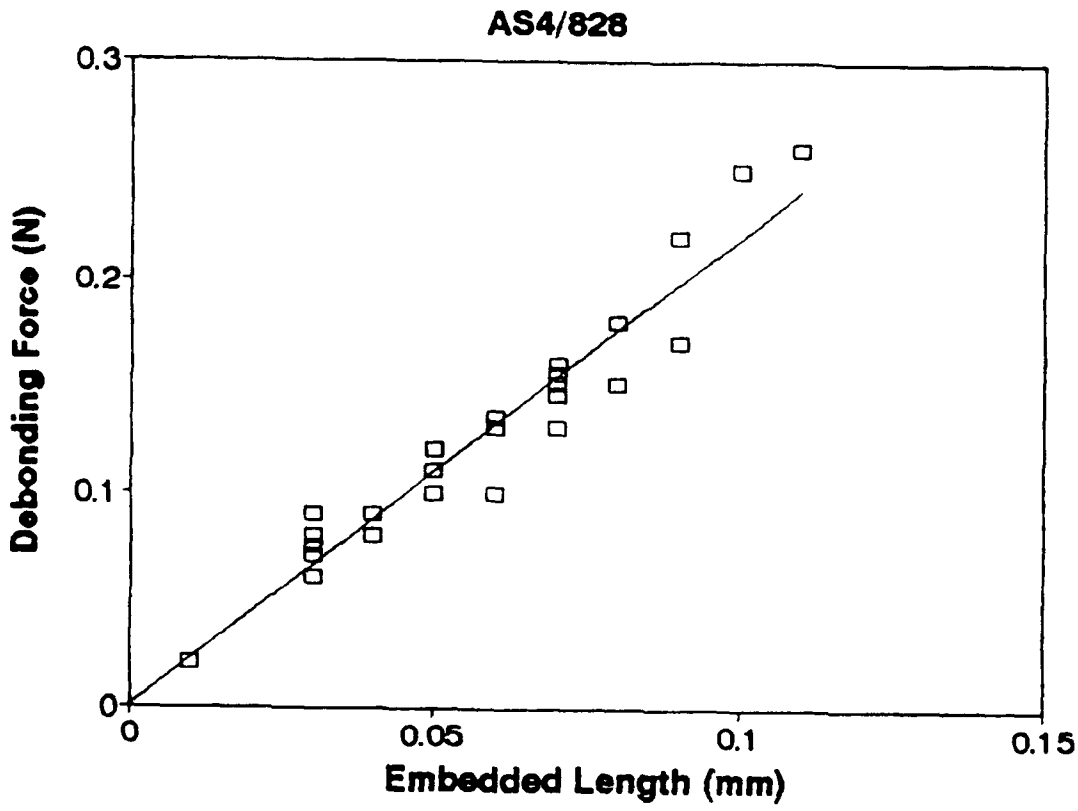

Fig. 5. Debonding force vs embedded length AS4/EPON 828, 135°C cure.

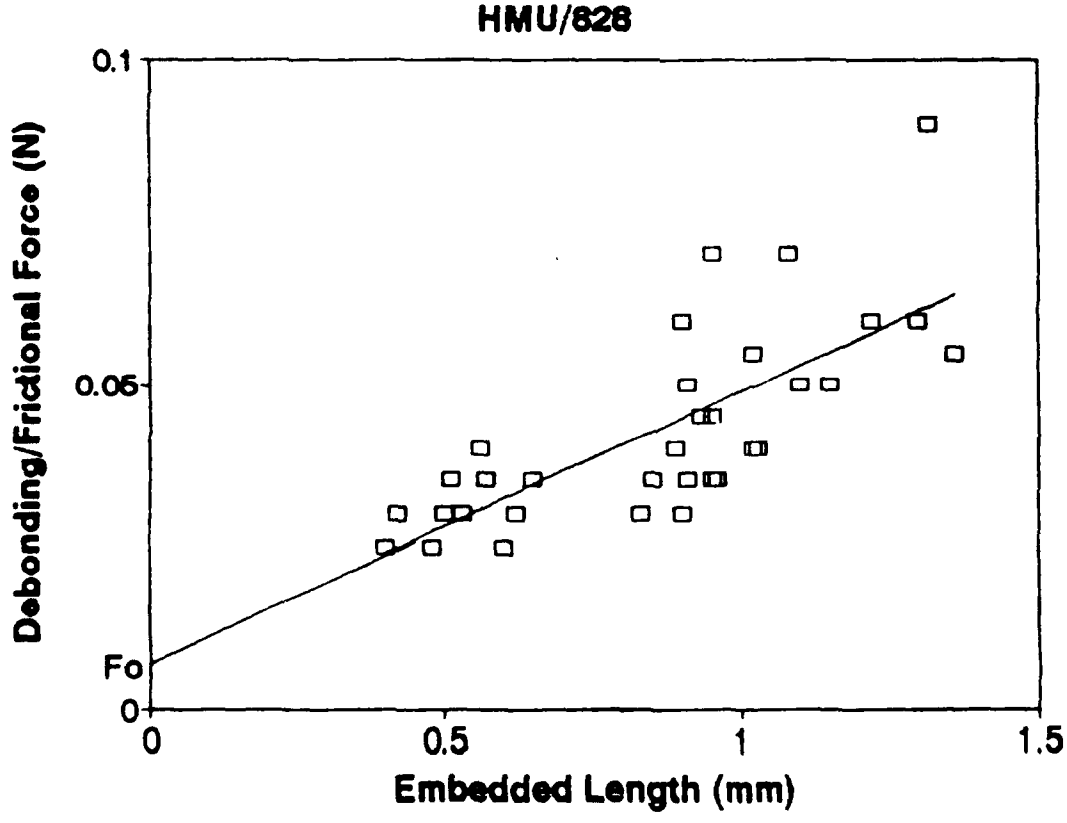

Fig. 6. Debonding and frictional vs embedded length HMU/EPON 828, 135°C cure.

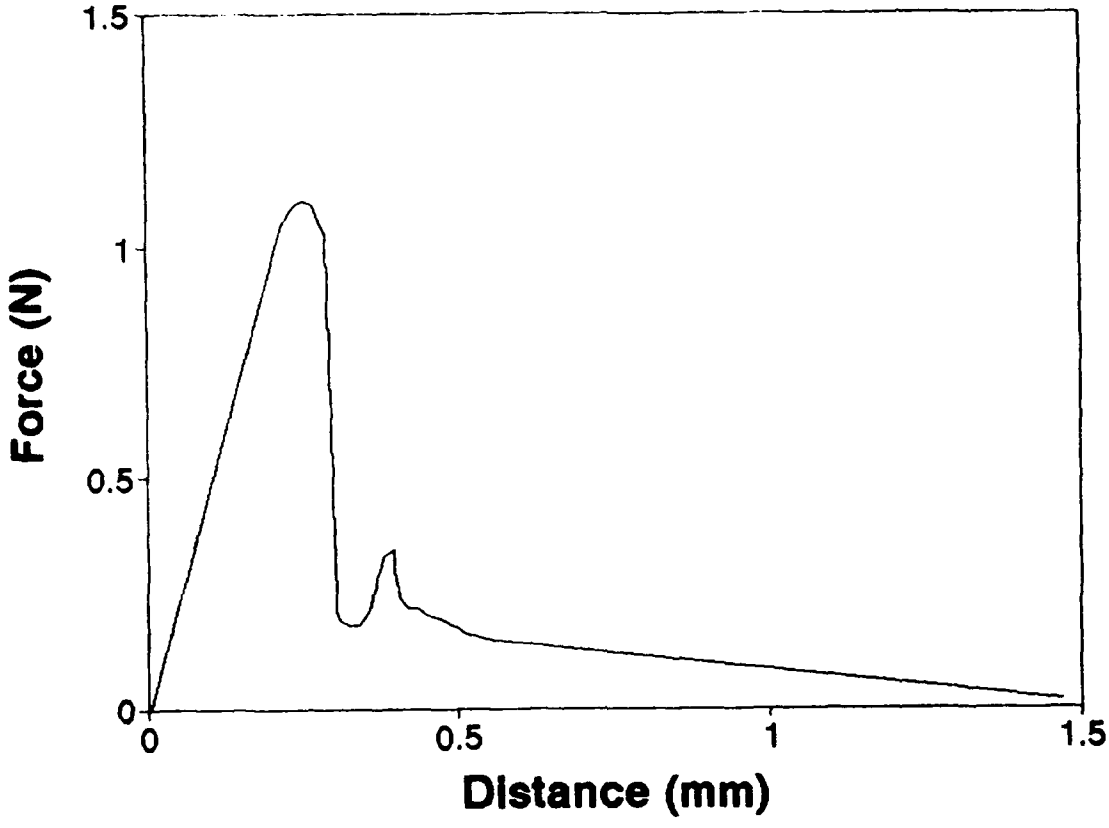

Fig. 7. Force vs distance moved during pull out: glass in LDPE.

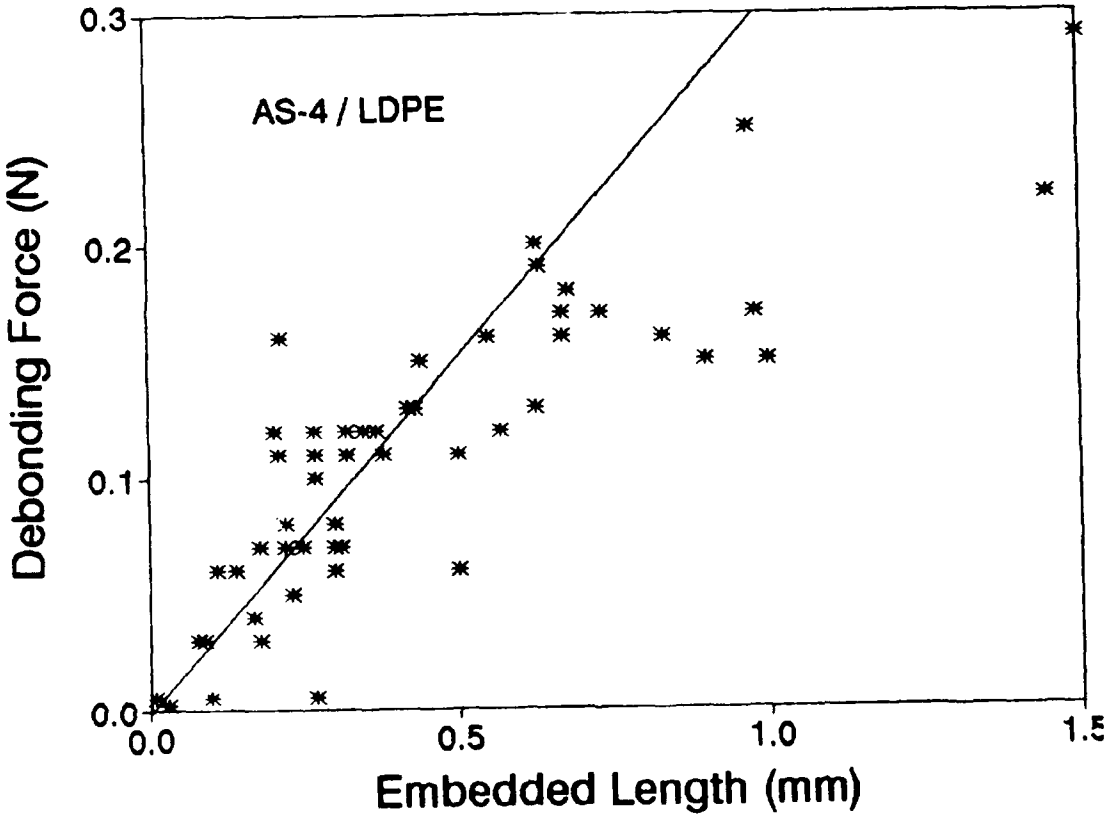

Fig. 8. Debonding force vs embedded length AS4 carbon in LDPE.

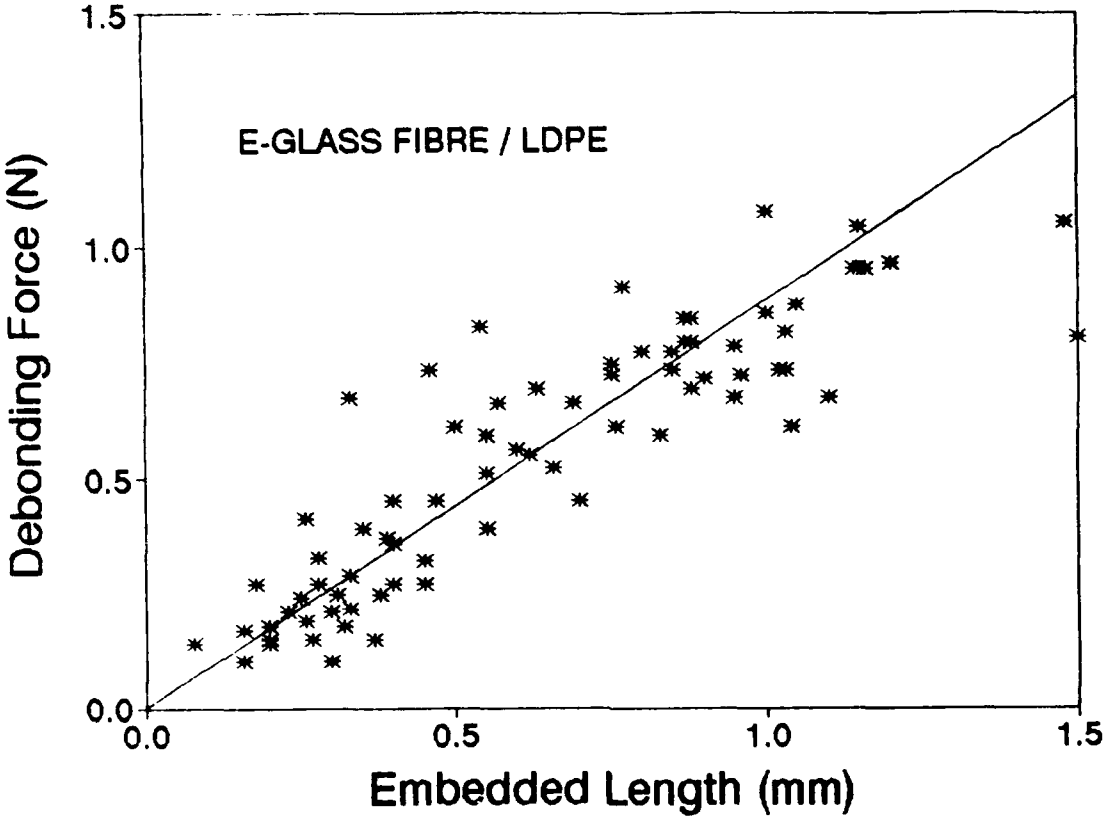

Fig. 9. Debonding force vs embedded length glass in LDPE.

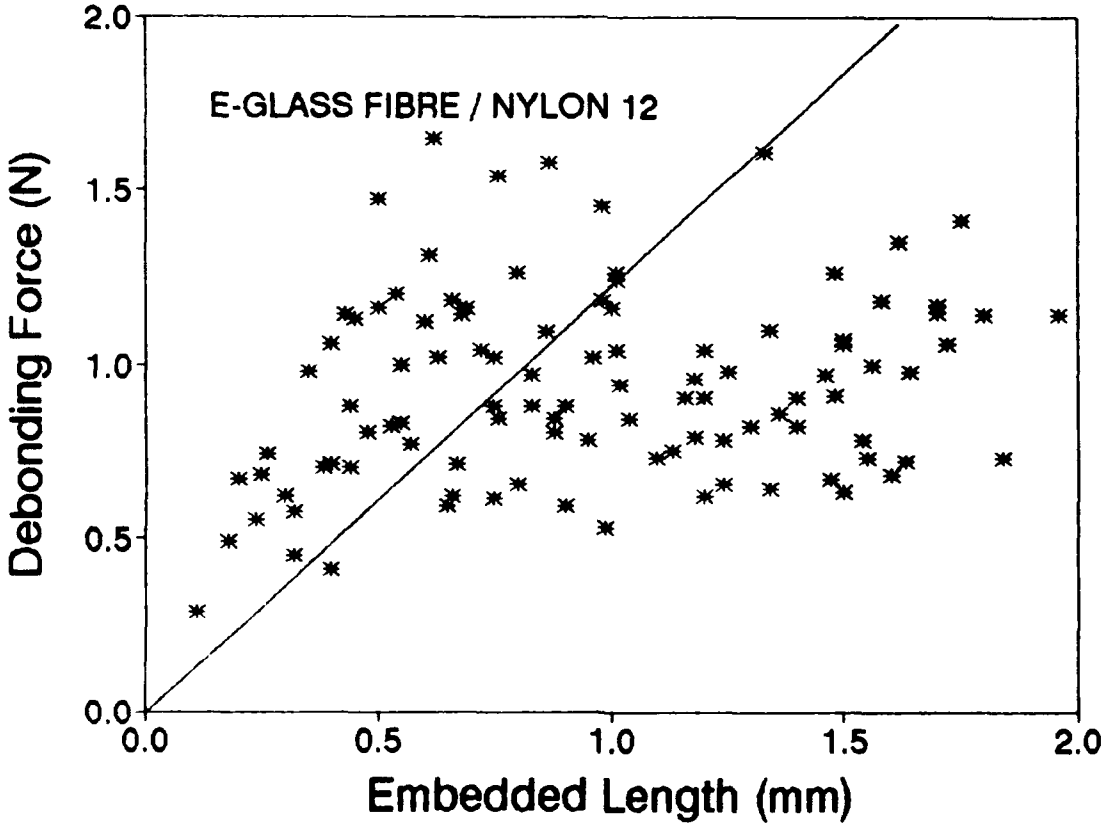

Fig. 10. Debonding force vs embedded length glass in nylon 12.

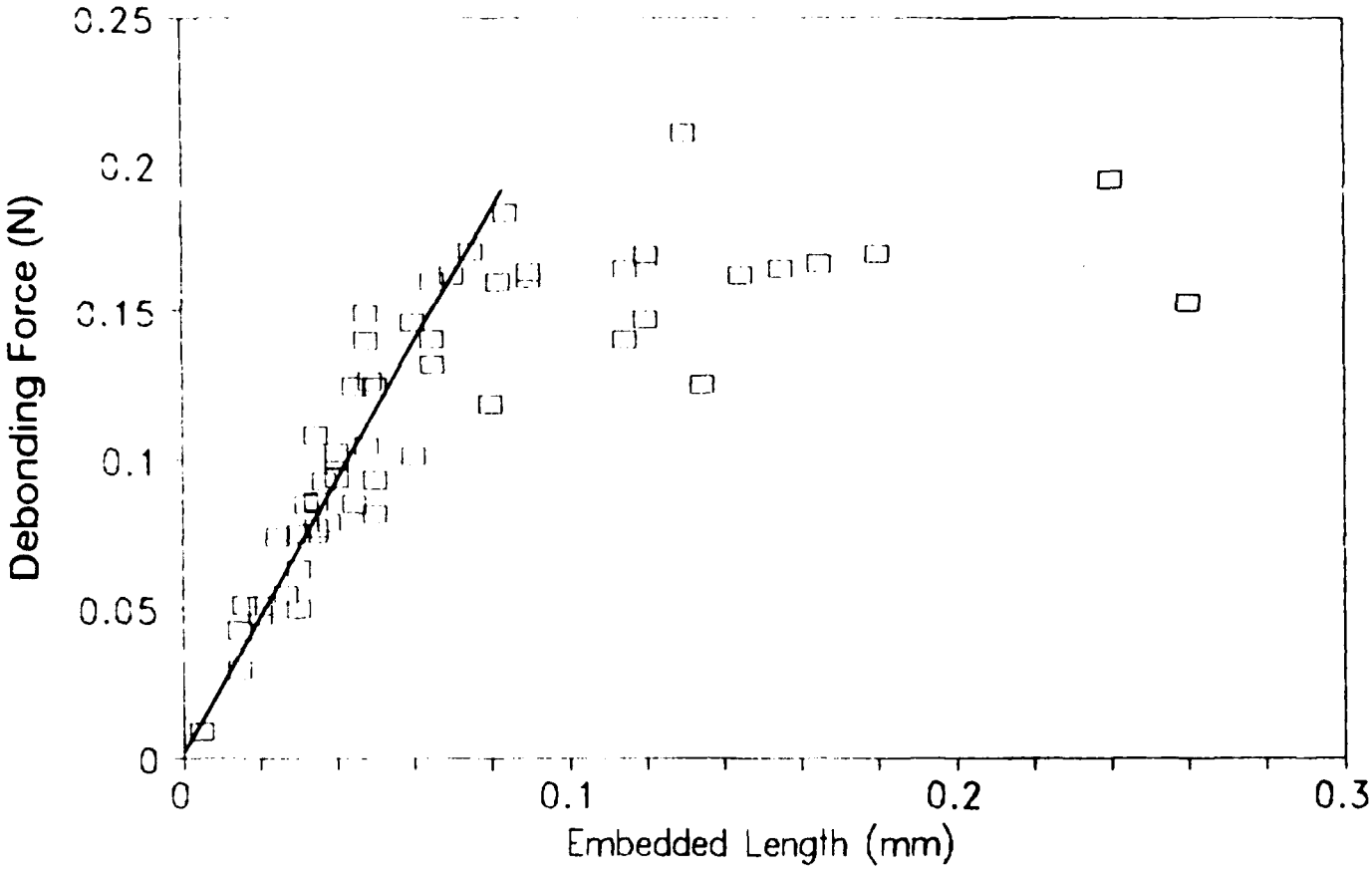

Fig. 11. Debonding force vs embedded length AS4 carbon in PEEK.

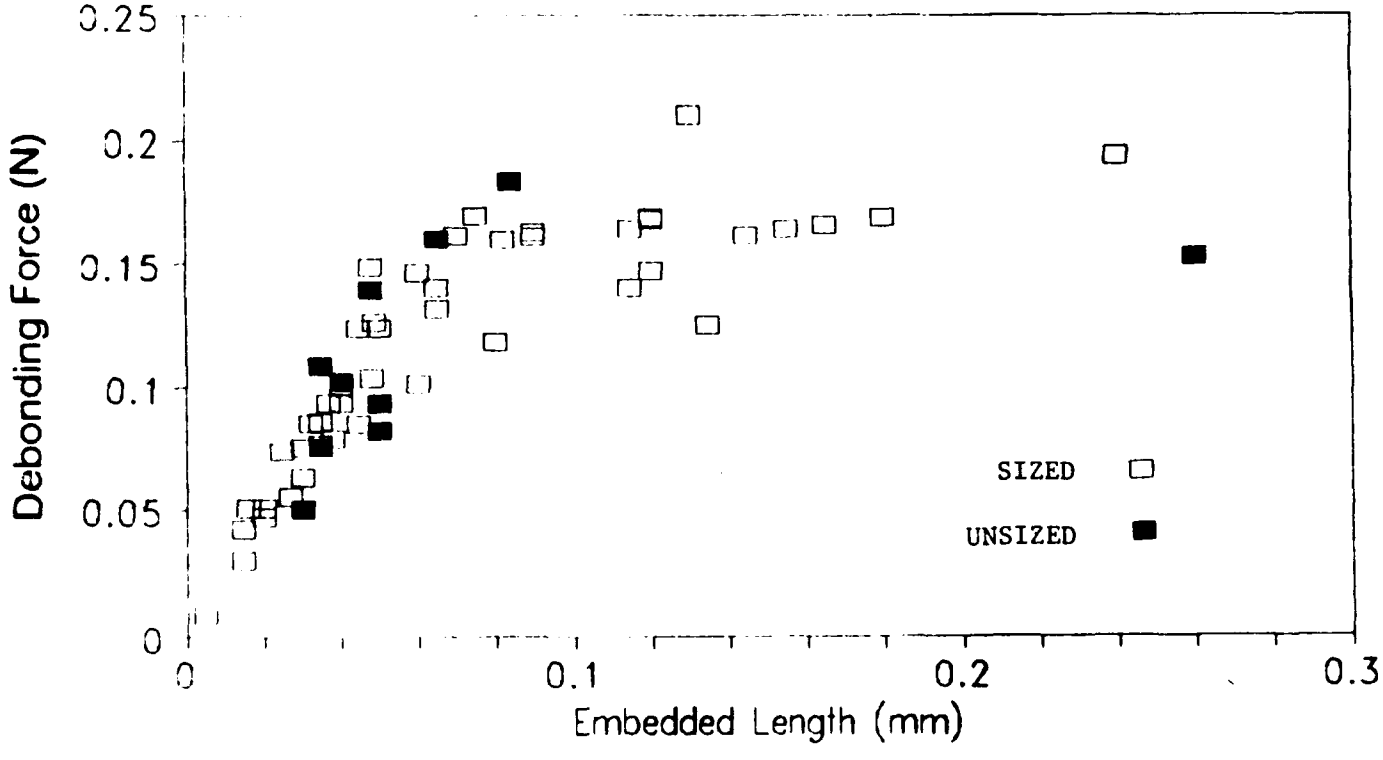

Fig. 12. Debonding force vs embedded length AS4 carbon in PEEK comparing sized (AS4) and unsized fibres.

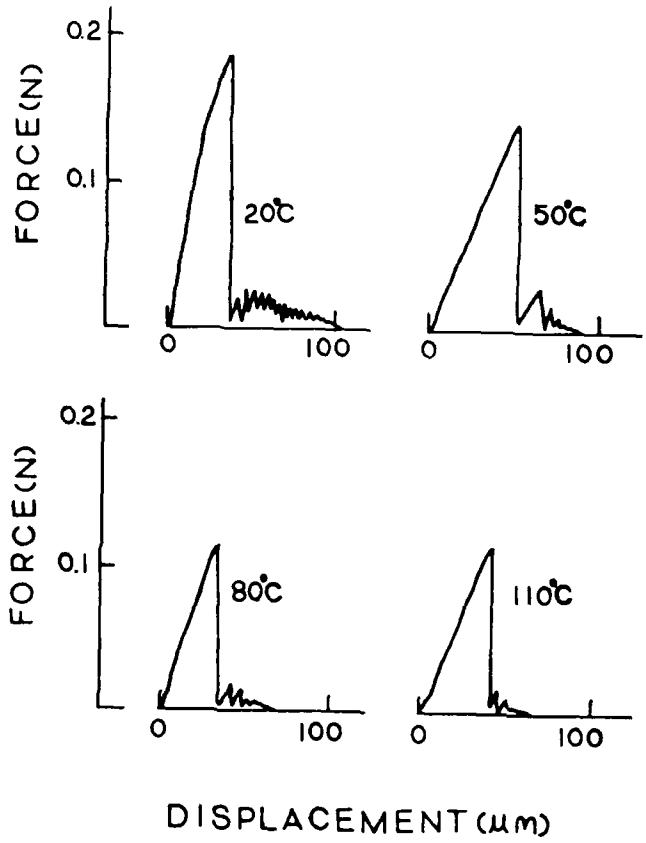

Fig. 13. Force vs distance moved during pull out: AS4 carbon in epoxy at four temperatures

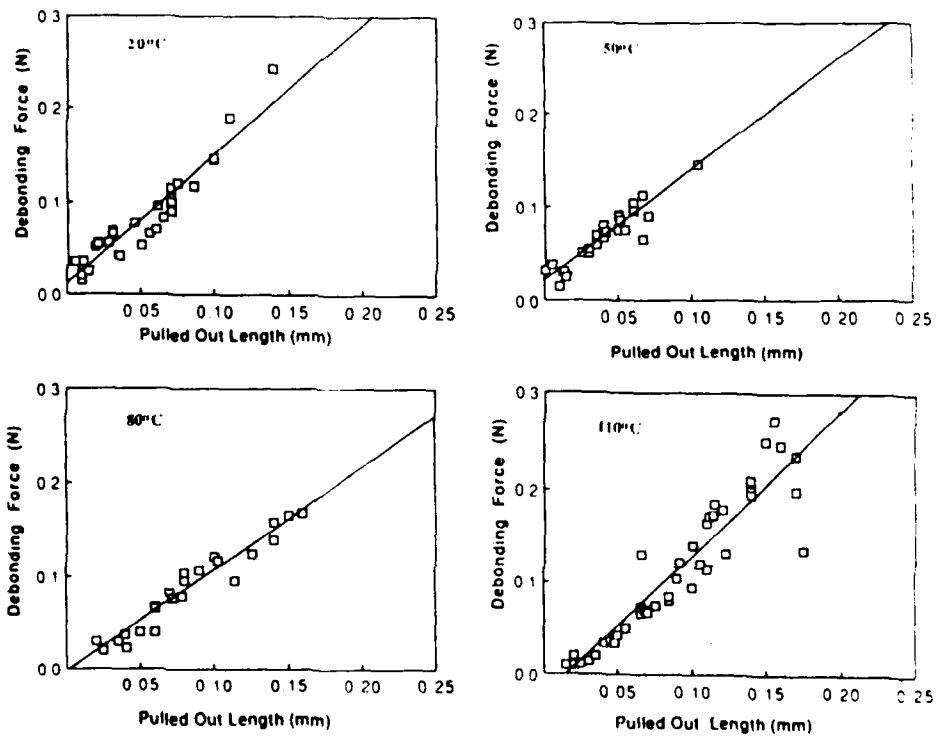

Fig. 14. Debonding force ve embedded length: AS4 carbon in epoxy at four temperatures

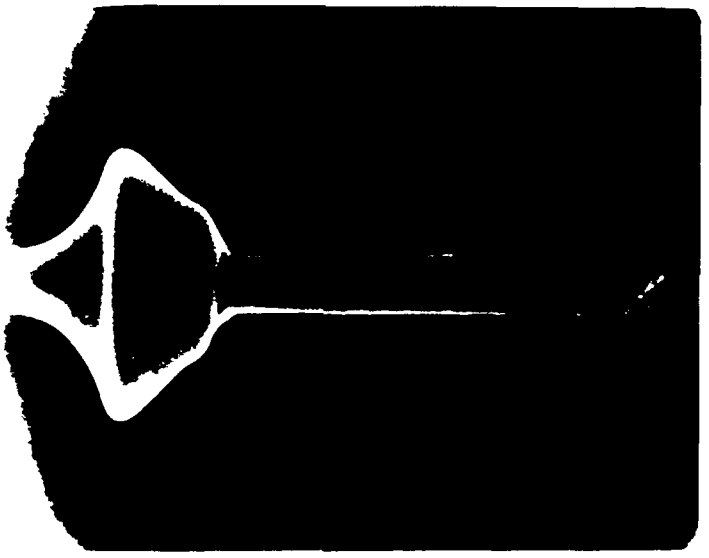

Fig. 15. Typical carbon fibre after being pulled out of epoxy at 50°C.

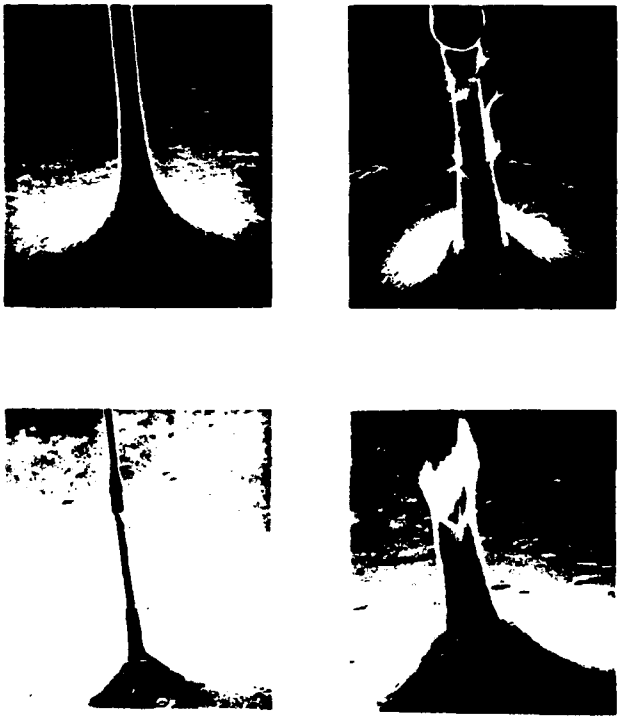

Fig. 16. Typical glass fibre being pulled out of LDPE.

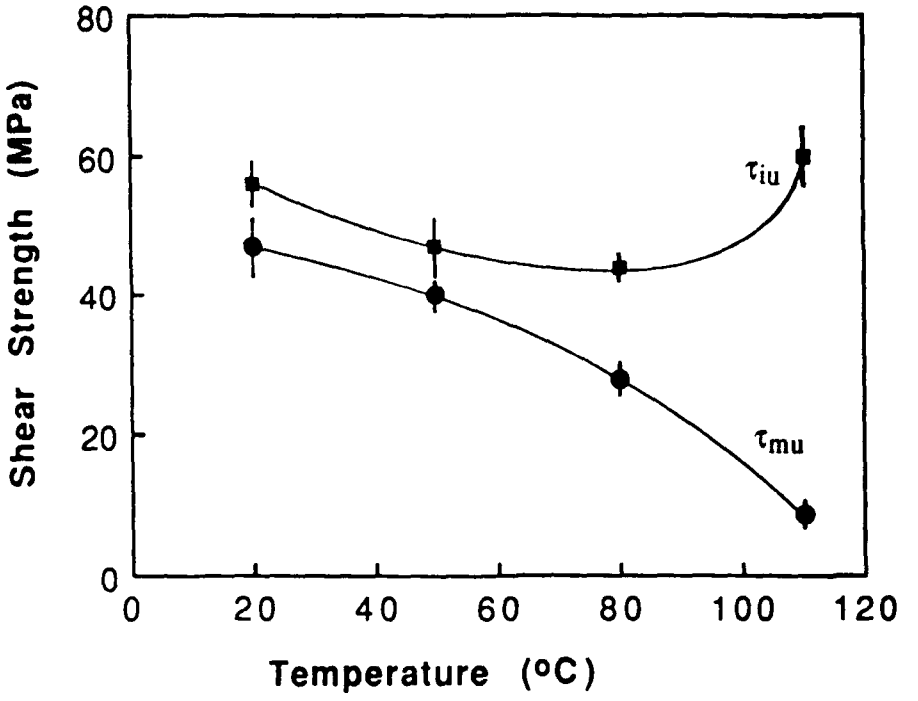

Fig. 17. Shear strength of interphase and polymer vs temperature.

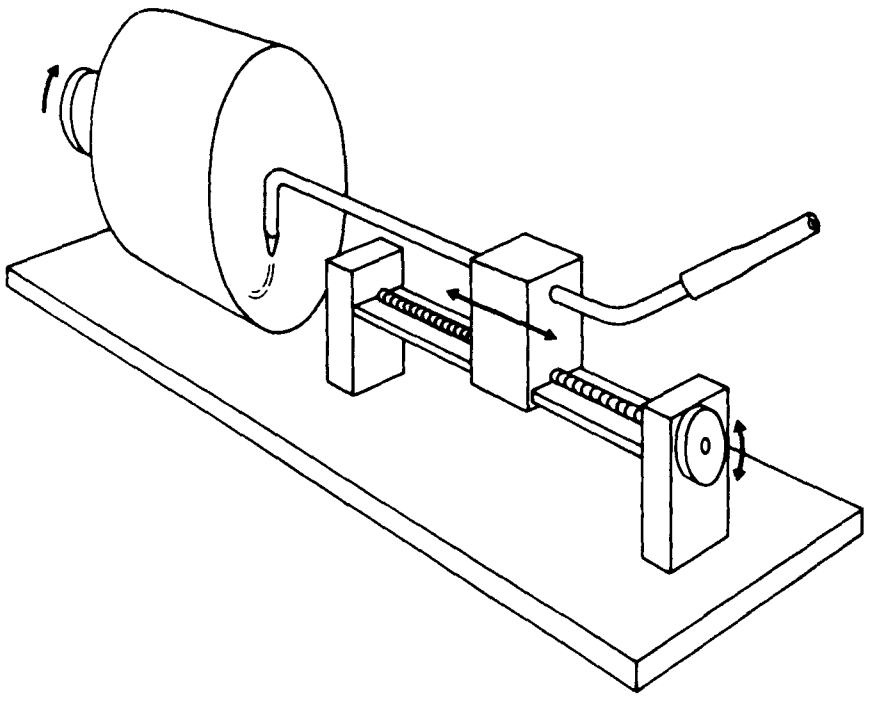

Fig. 18. Schematic drawing of the machine used for fibre alignment.

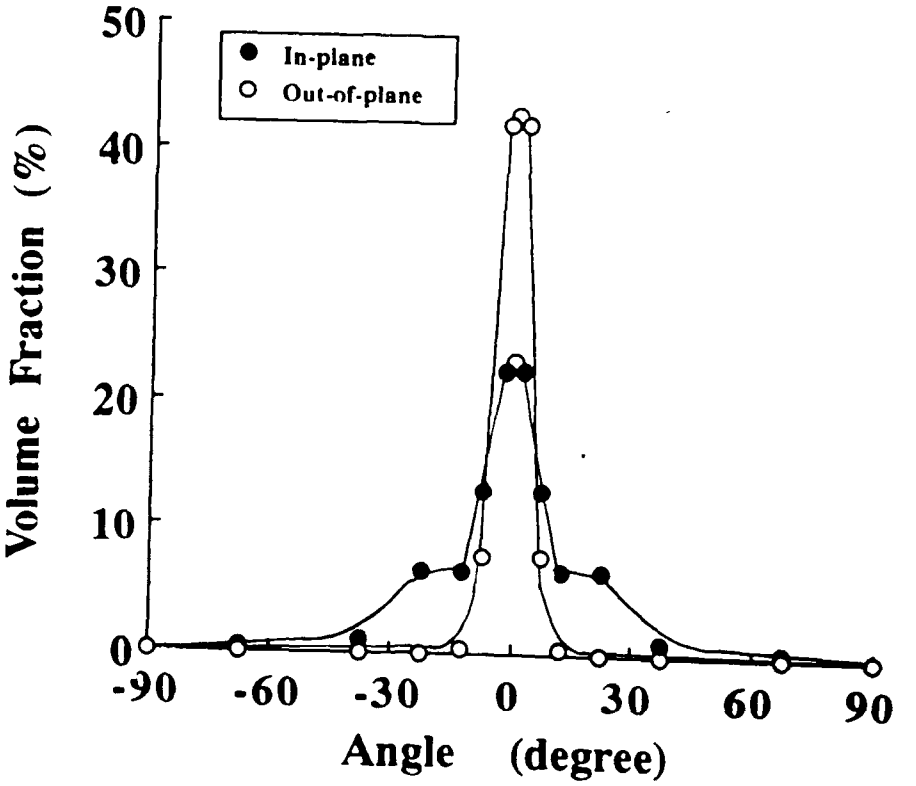

Fig. 19. Fibre angle distribution for 2 mm fibres.

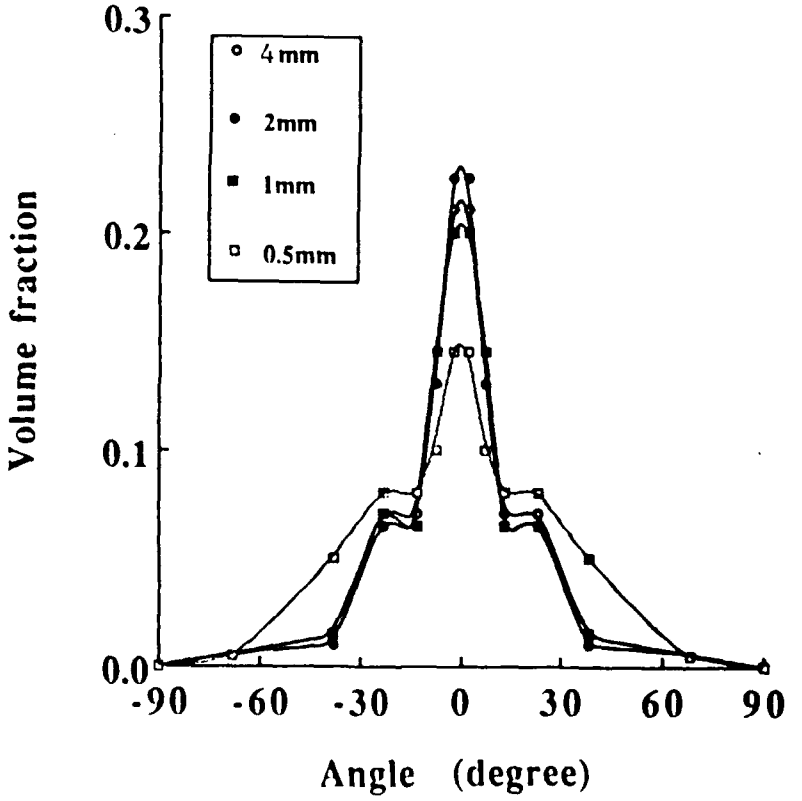

Fig. 20. In plane angular distributions for fibres in composites.

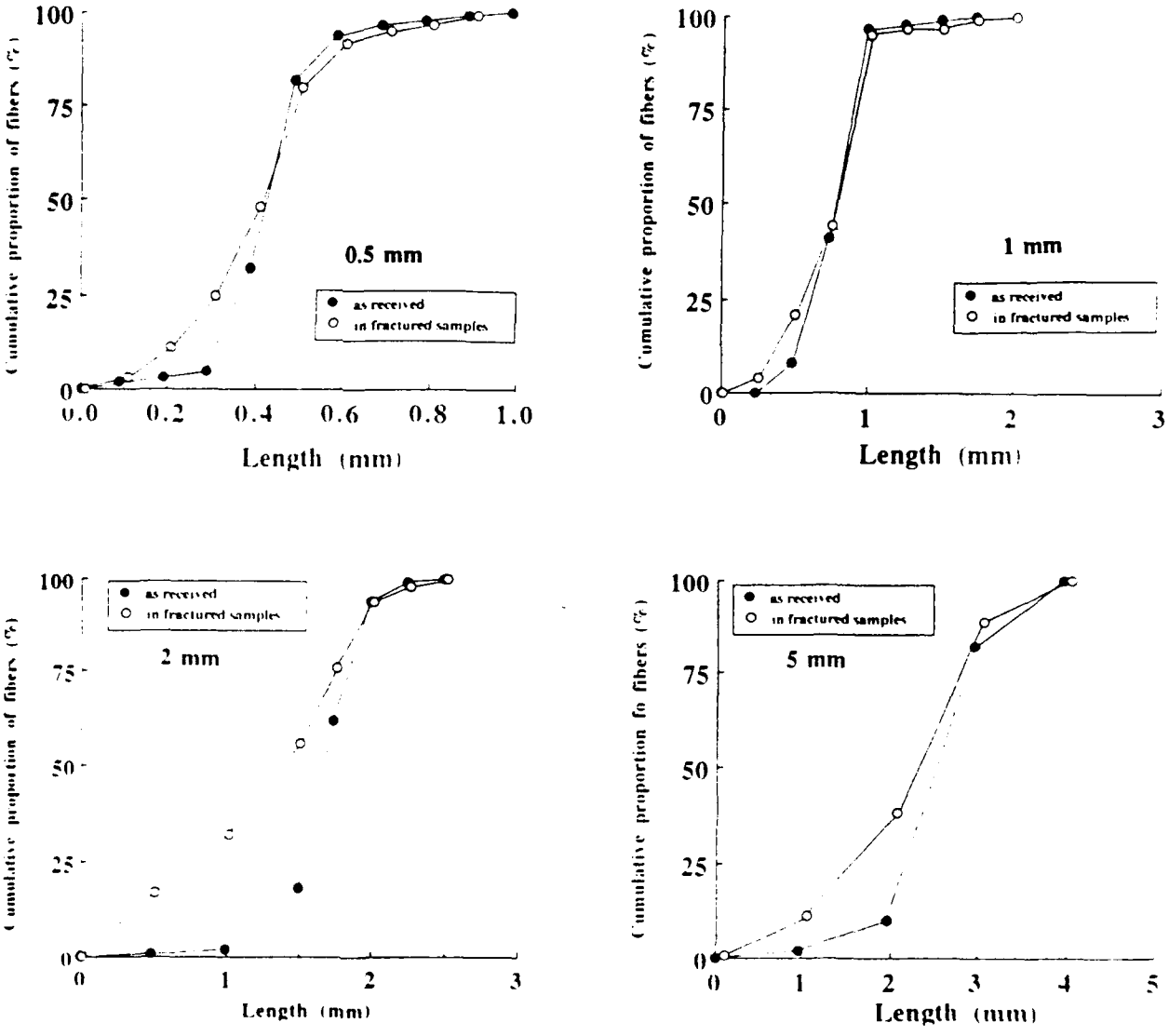

Fig. 21 Fibre lengths measured as received and after extraction from composites, for nominal fibre lengths of 0.5, 1.0, 2.0 and 5.0 mm.

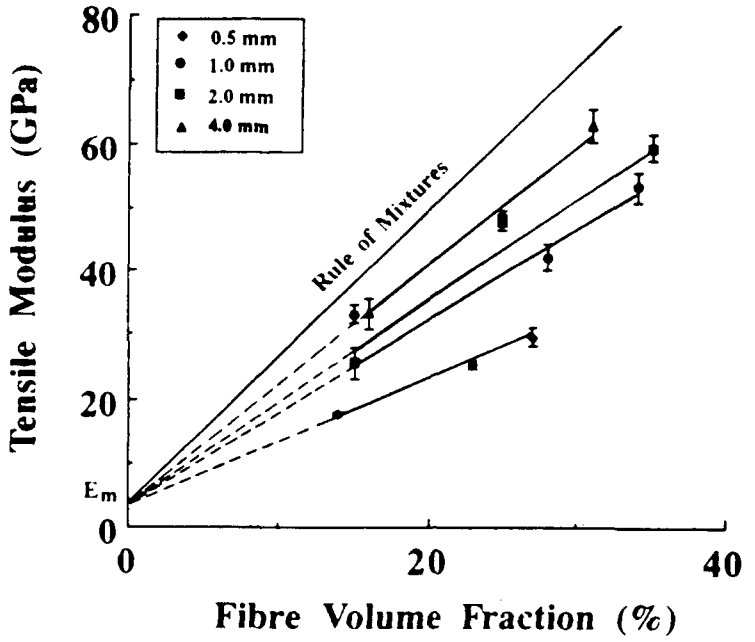

Fig. 22. Young's moduli of carbon fibre reinforced epoxy. Nominal fibre lengths 0.5, 1.0, 2.0 and 4.0 mm as indicated.

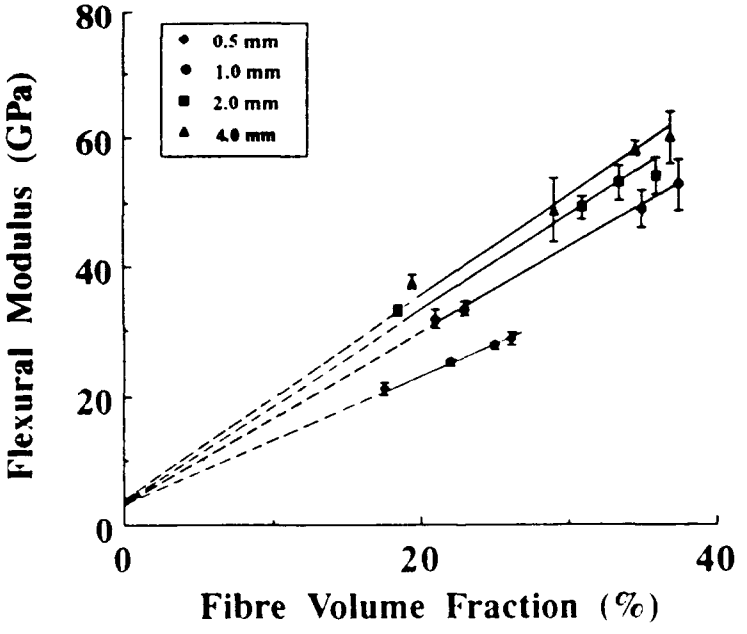

Fig. 23. Flexural moduli of carbon fibre reinforced epoxy. Nominal fibre lengths 0.5, 1.0, 2.0 and 4.0 mm as indicated.

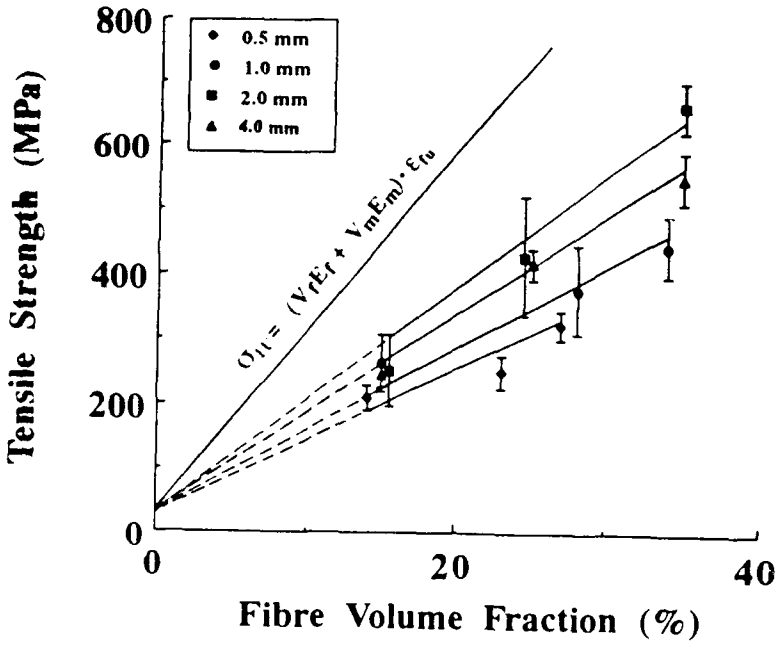

Fig. 24. Tensile strengths of carbon fibre reinforced epoxy. Nominal fibre lengths 0.5, 1.0, 2.0 and 4.0 mm as indicated.

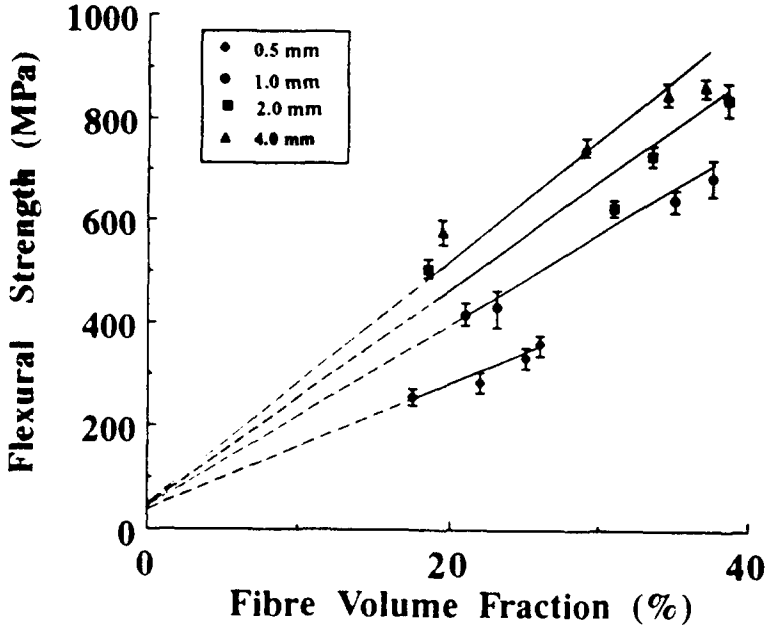

Fig. 25. Flexural strengths of carbon fibre reinforced epoxy. Nominal fibre lengths 0.5, 1.0, 2.0 and 4.0 mm as indicated.

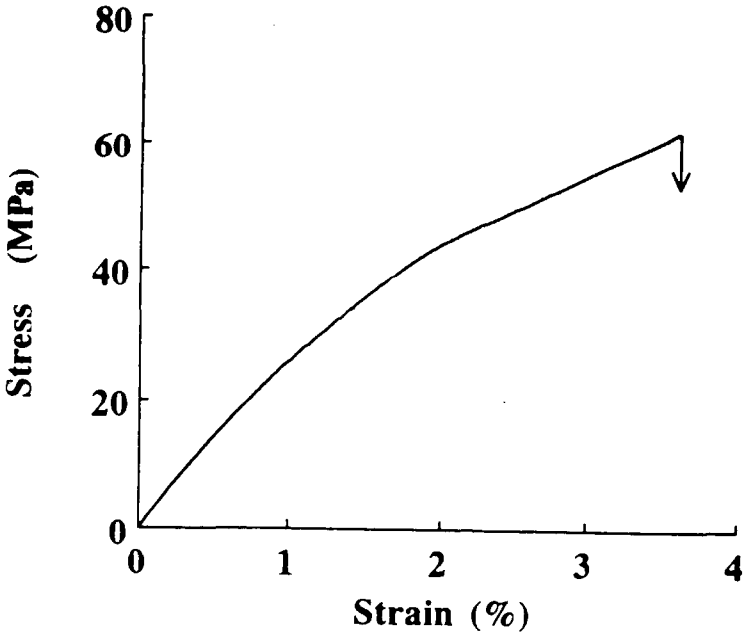

Fig. 26. Stress strain curve for epoxy resin matrix.

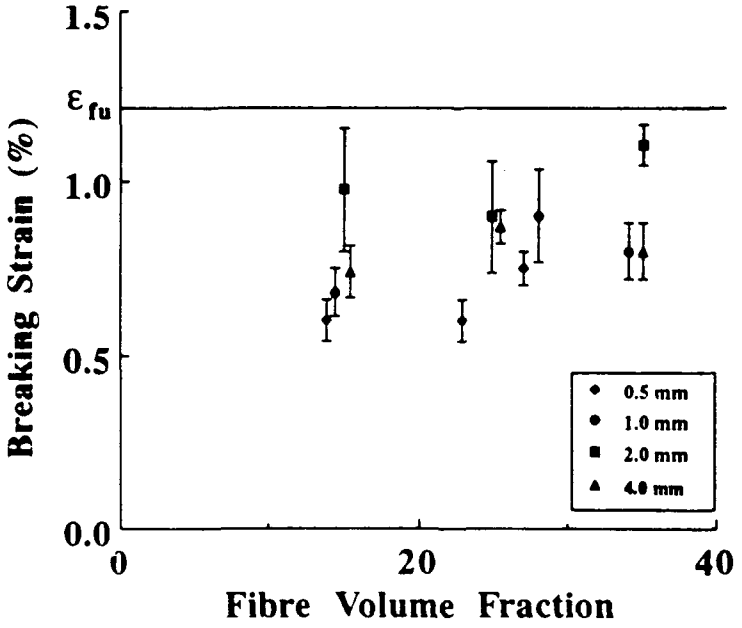

Fig. 27. Breaking strains of fibre composites

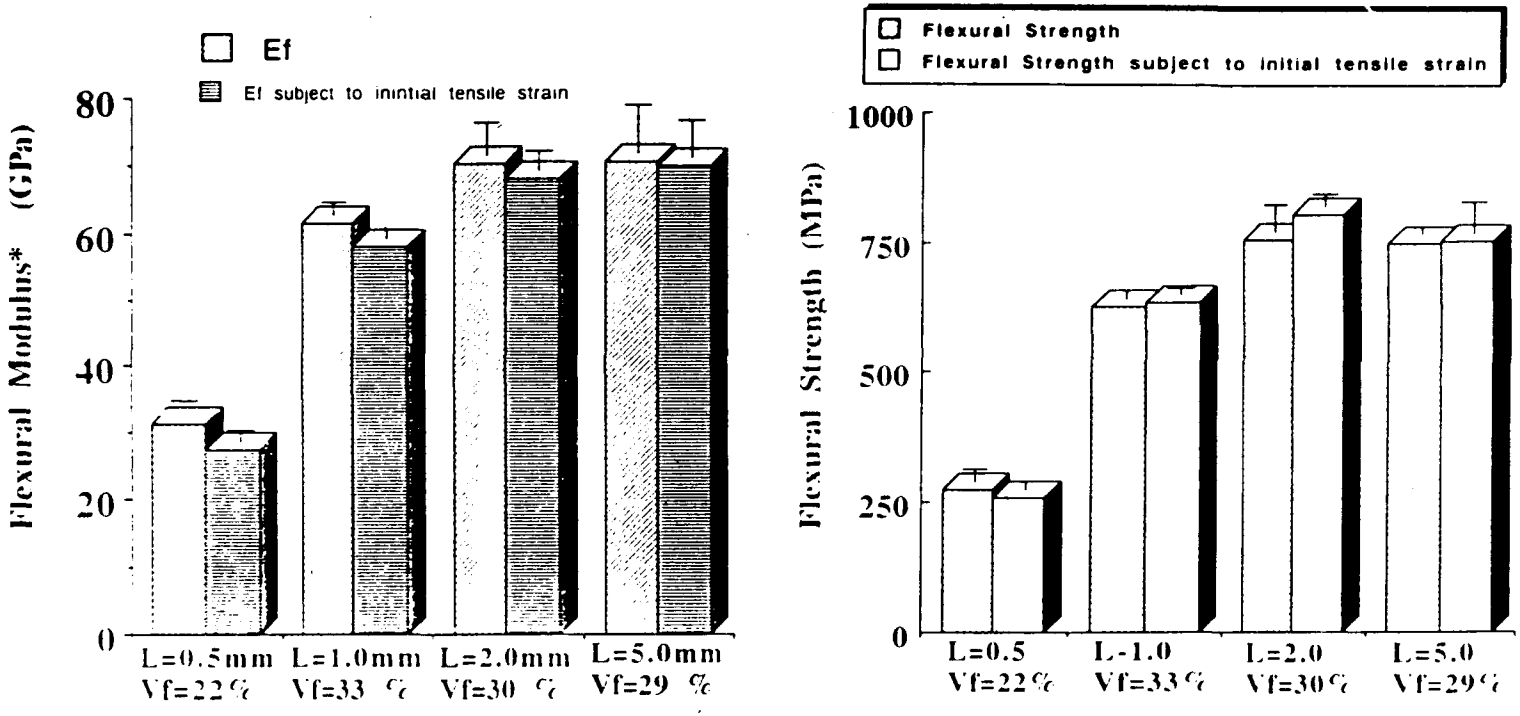

Fig. 28. Changes in flexural modulus and strength for prestrained composites

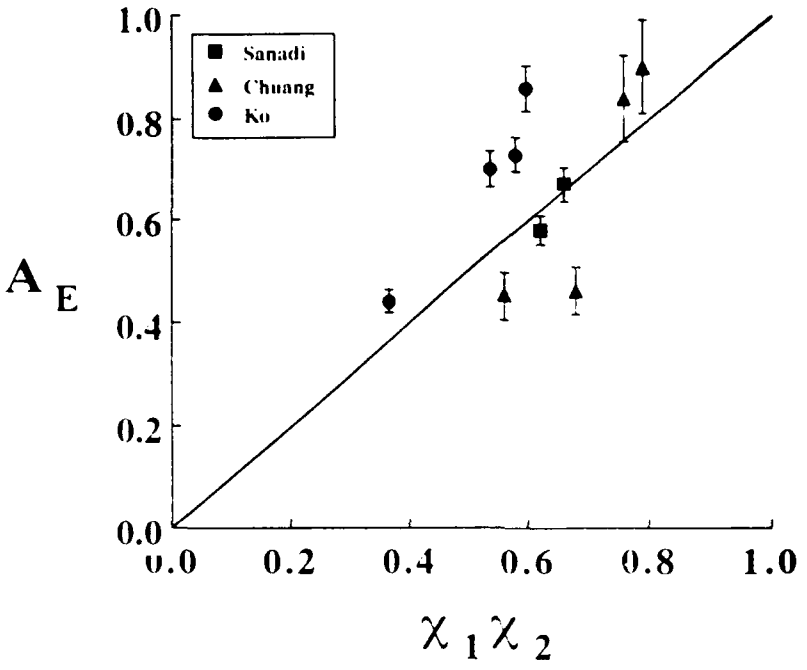

Fig. 29. Modulus reduction factor for short fibre composites, comparing previous work [8,9] and this work [Ko].

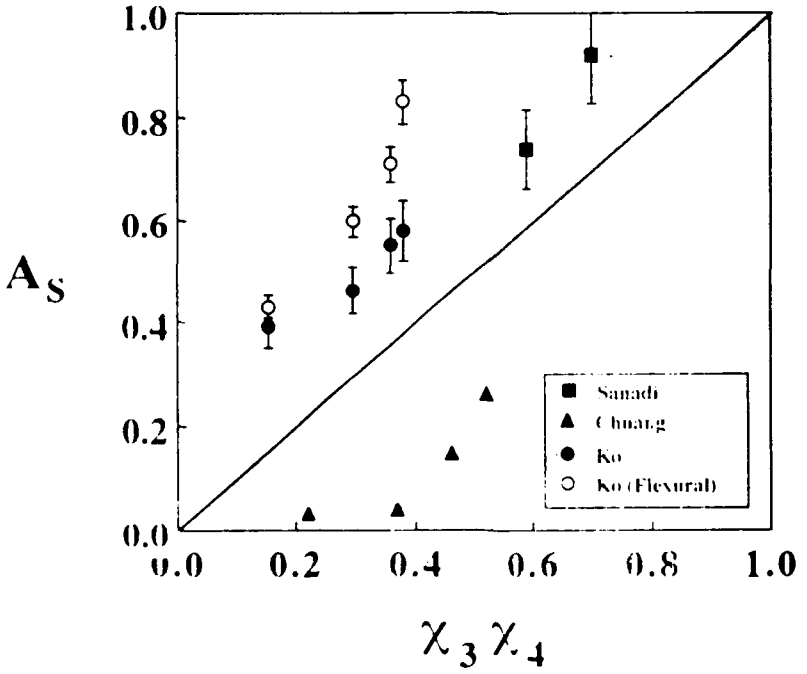

Fig. 30. Strength reduction factor for short fibre composites, comparing previous work [8,9] and this work [Ko].

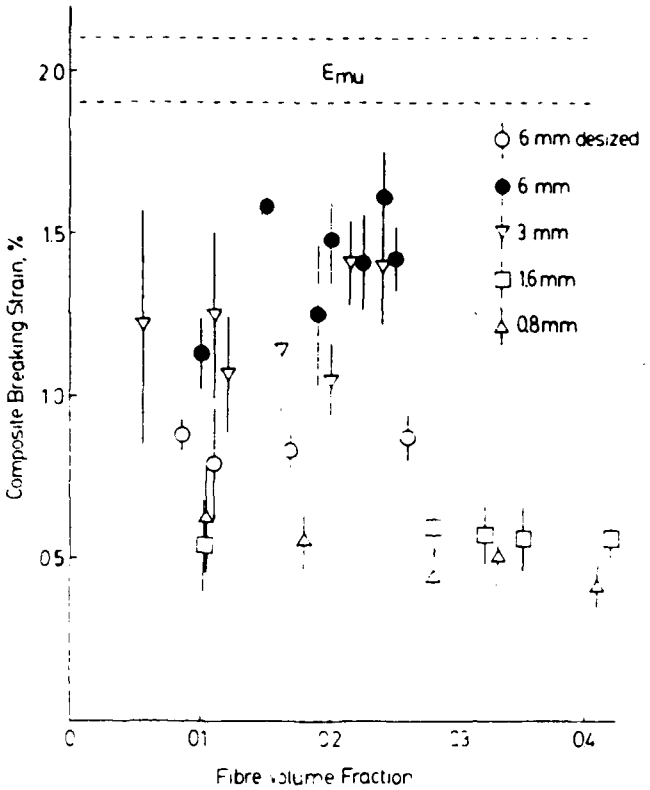

Fig. 31. **Breaking strains for glass epoxies [9].**

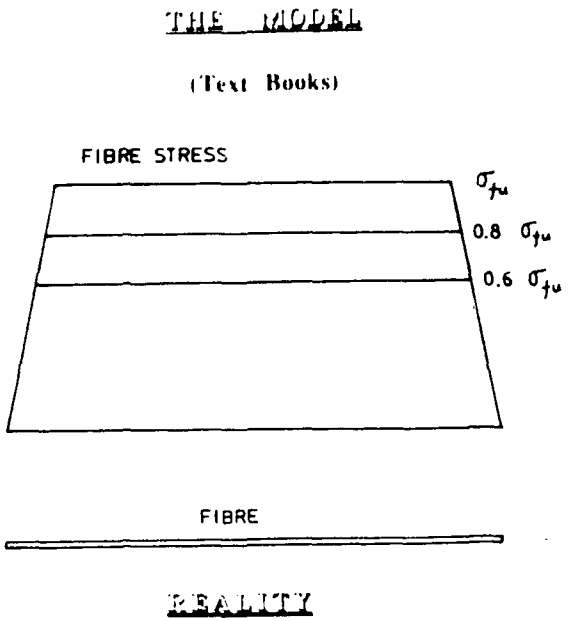

(Galiotis. Comp. Sci. Tech. 42 (1991), 125-50)

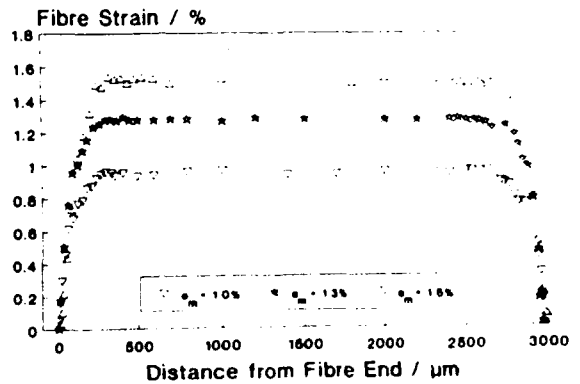

Fig. 32. Ductile interface model compared [11] with laser RAMAN data [12].